

QUILL

Quarterly Reports



May - July 2019



Contents

Non-Aqueous Electrolytes for Flow Batteries (Robert Boyd)	3
Physical Characterisation of Functional Liquids (Emily Byrne)	7
Microemulsion Solvent Systems for Bio-Separations (Martyn Earle).....	11
Gas Line Design for the NMR Study of Ethane and Ethylene Absorption (David Greene).....	21
Encounter complexes in Frustrated Lewis Pairs (Anne McGrogan).....	25
Production of Alkyl Levulinates using Hybrid Organic-Inorganic materials based on Polyoxometalates and Ionic Liquids (Lucia McLaughlin)	29
Base Stable and Basic Ionic Liquids (Peter McNeice)	38
Investigation of Pd(II) Catalysed Oxidation Reactions (Rebecca Millar)	43
Ionic Liquid Catalysts for the Glycolysis of PET (Gareth Nelson)	49
Developing New Nanocatalysts for the Direct Conversion of Biogenic Carbon Dioxide (CO ₂) to Sustainable Fuels (Zara Shiels).....	51



QUILL Quarterly Report

May 2019 – July 2019

Name:	Robert Boyd		
Supervisor(s):	Peter Nockemann, Martin Atkins		
Position:	Final year PhD		
Start date:	September 2016	Anticipated end date:	February 2020
Funding body:	DEL		

Non-Aqueous Electrolytes for Flow Batteries

Background

Cheap, safe and efficient energy storage is essential in developing practical and sustainable energy strategies necessary for maintaining a balanced, efficient and reliable electric grid system based on both conventional electricity generation industries and the integration of intermittent renewable energy sources.

Batteries for large-scale grid storage must satisfy a different set of variables compared to many conventional rechargeable batteries. Such batteries must be; durable, maintain efficiency over a large number of charge/discharge cycles, have high round-trip efficiency, able to respond instantly to changes in load or input, and have reasonable capital costs^[1]. Redox flow batteries are able to meet much of this criterion hence there has been significant interest in the optimisation of redox flow batteries for large-scale energy storage over the last few decades.

The all vanadium RFB was and remains the 'flagship' for redox flow batteries. It has a higher energy efficiency, longer operational lifetime and lower cost compared with other redox batteries (zinc bromide, sodium sulfur and lead acid)^[2]. It remains the only RFB to have been sold in significant numbers due in part to being the only RFB to make use of the same metal species in both half-cells, avoiding cross-contamination issues.

Flow batteries incorporating organic molecules as the charge carriers are experiencing significant interest for large scale energy storage. Engineering the structure of organic molecules can deliver low cost redox active molecules with favourable potentials, increased solubility and greater stability. Both quinones and N-heterocycles are currently experiencing extensive investigation for application in flow batteries.

Objective of this work

Improve upon the commercial all-vanadium battery by reducing costs, increasing energy density and increasing cell voltage.

Progress to date

Anthraquinone

Anthraquinones are planar molecules featuring three cyclic rings and two carbonyl groups which can store two electrons per molecule.

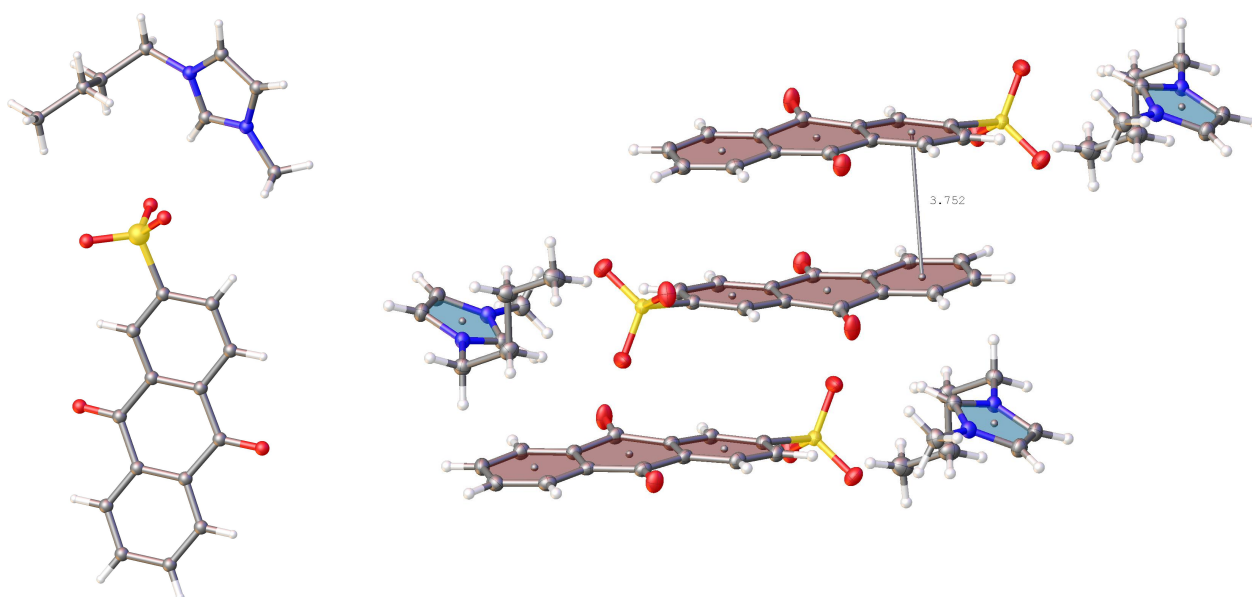


Figure 1 - Crystal structures showing the [C₄mim][AQS] ion pair and the packing of the ionic compound with the quinone planes coloured red and imidazole planes coloured blue.

Single crystal measurements reveal layers of anthraquinone, 3.752 Å apart, originating from pi-pi intermolecular interactions. This compact, ordered structure makes it difficult to dissolve or liquify, reducing energy density.

To overcome low solubility, the phosphonium cation [P₆₆₆₁₄] was incorporated as the cation to add disorder and resulted in the formation of a viscous yellow liquid, density = 1.0394 g mL⁻¹ at 20 °C, which could be easily dissolved in organic solvents.

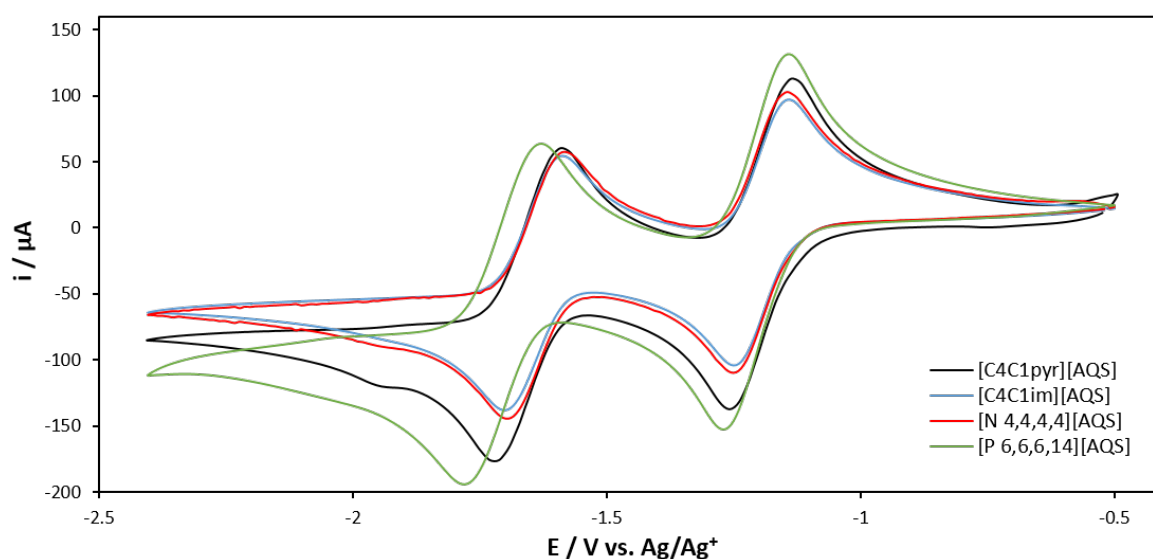


Figure 2 - CVs of four anthraquinone sulfonate compounds featuring a pyrrolidinium, imidazolium, ammonium and phosphonium cation.

Anthraquinone undergoes two consecutive reversible, single electron reductions forming the radical anion^[3] and dianion, stabilised through its resonance forms. Altering the cation had little

effect on the position of the peaks associated with the formation of the quinone radical however the peaks corresponding to the dianion were shifted towards more negative values for the pyrrolidinium and phosphonium derivative potentially due to the unstable nature of the two negative charges.

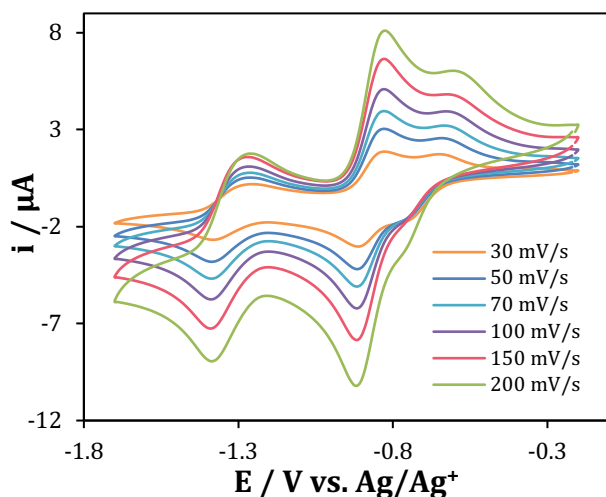


Figure 4 - CV of $[C_1C_4pyr][AQS]$ in $[C_1C_4pyr][NTf_2]$ at various scan rates.

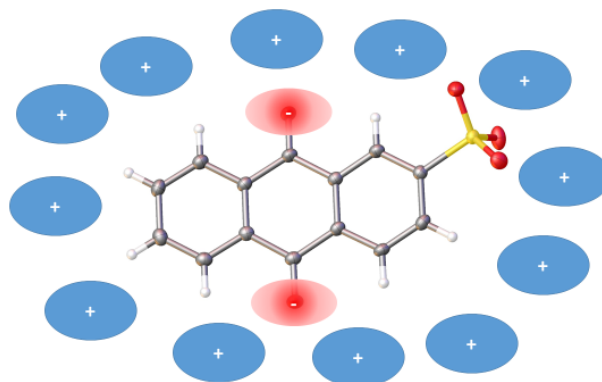


Figure 3 - Diagram of dianion in ionic liquid solvent.

Using ionic liquid as a solvent failed to significantly increase the solubility of the pyrrolidinium derivative however changes in electrochemical behaviour were observed. Peaks were shifted to more positive values due to the improved stability of redox products in the ionic liquid. Lower current values were displayed due to the viscous nature of ionic liquid with the dianion oxidation peak appearing disproportionately lower than the others. This can be explained by the large increase in electron density on formation of the dianion which interacts with solvent cations reducing mass transfer, limiting the number of molecules able to reach the electrode.

Hydroquinone

Hydroquinone compounds were synthesised to compliment anthraquinones as the catholyte.

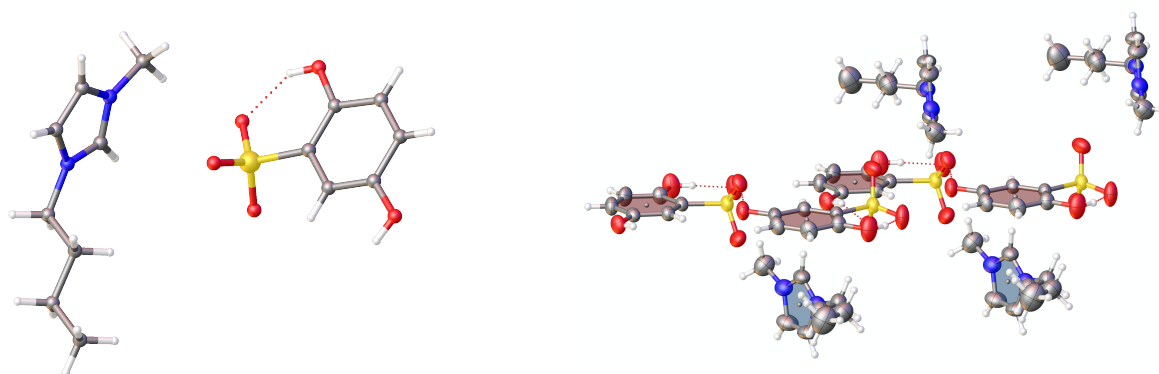


Figure 5 - Crystal structure of $[C_4mim][AQS]$.

Hydroquinone appears to show a much less closely packed crystal structure, increasing solubility relative to anthraquinone.

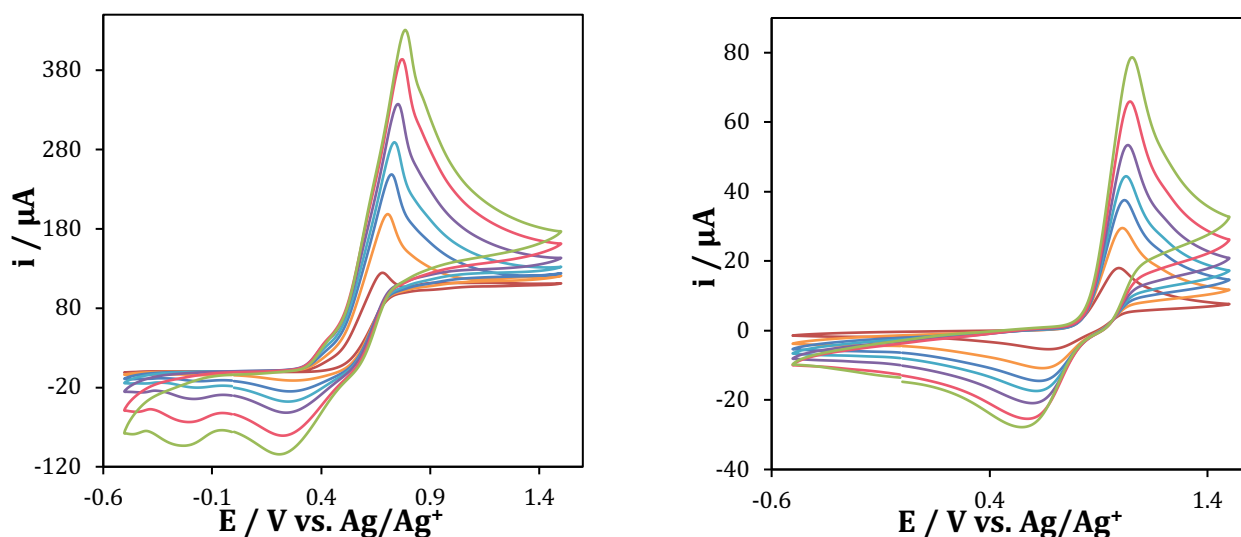


Figure 6 - CVs of $[C_4C_1pyr][HQS]$ in acetonitrile with $[NEt_4][BF_4]$ (0.1 M) (left) and $[C_4C_1pyr][NTf_2]$ (right).

Cyclic voltammetry revealed irreversible electrochemistry indicated by the distance between both peaks. The addition of acid resulted in both peaks shifting to higher potentials however the reduction peak shifted significantly more to become an electrochemically reversible process.

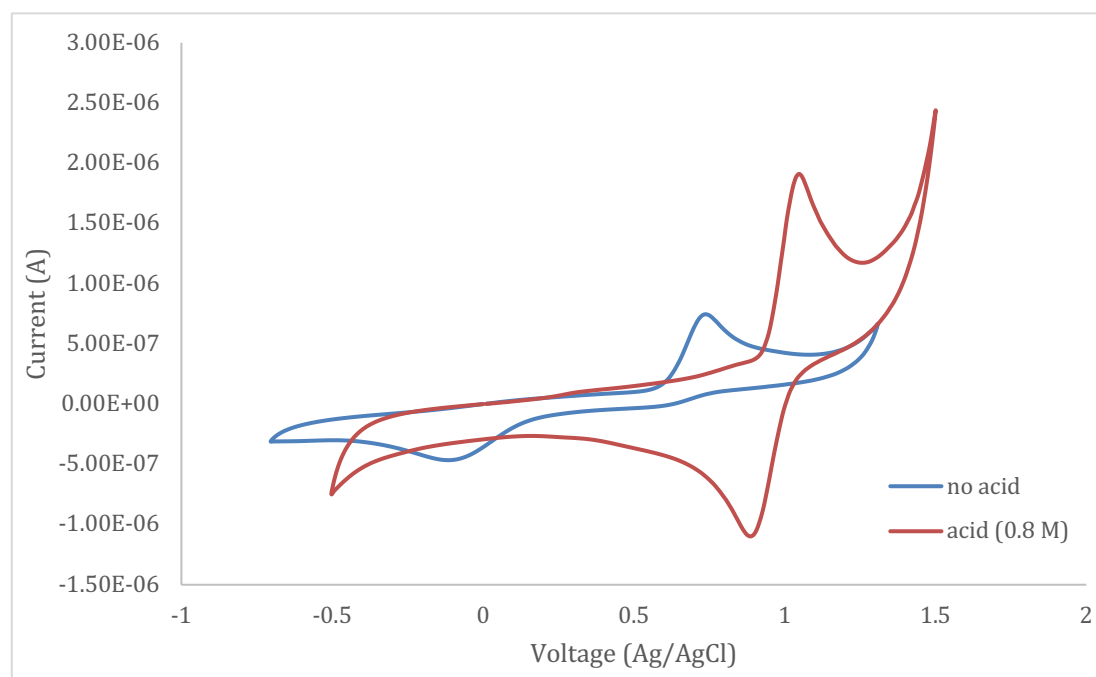


Figure 7 - $[P_{66614}][HQS]$ in $[P_{66614}][NTf_2]$ neat and with $HNTf_2$ (0.8 M) added. Both scans ran at 10 mVs^{-1} .

Conclusions and future work

Quinones incorporated into ionic liquids display reversible electrochemical behaviour provided a small amount of acid is present in the hydroquinone system. A complete cell should be possible using an anthraquinone and hydroquinone together. Future work will involve the use of these ionic liquids to form a membrane-free, 2-phase battery as well as conventional membrane separated batteries.



QUILL Quarterly Report

May - July 2019

Name:	Emily Byrne		
Supervisor(s):	Dr Małgorzata Swadźba-Kwaśny and Prof John Holbrey		
Position:	PhD student		
Start date:	October 2017	Anticipated end date:	October 2020
Funding body:	DfE (Department for the Economy)		

Physical Characterisation of Functional Liquids

Background

It is proposed that deep eutectic solvents 'DES' are a chemical component mixture composed of hydrogen bond donors and acceptors which have intermolecular interactions that result in a freezing point which is lower than that of the isolated individual components of the system with no interactions between each other.¹ They are asymmetric species which, due to their orbitals' inability to overlap well and thus, pack into a regular lattice arrangement, have low lattice energy and so do not require a large amount of energy in order to exist as a liquid and as a result tend to have low melting points.

The most common and well renowned DES are those prepared with the combination of organic salts such as choline chloride, which act as a hydrogen bond acceptor and carboxylic acids or alcohols with a hydrogen bond donating role.²⁻⁵ However, these solvents are generally miscible with water and so their application is quite limited. Therefore, work was undertaken by van Osch *et al.* which led to the publication of the first hydrophobic deep eutectic solvent using a carboxylic acid hydrogen bond donor and a long chain quaternary ammonium salt in 2015.⁶ In addition to this, DES have since been formed using alcohols and fatty acid hydrogen bond donors in combination with organic salts to form deep eutectic solvents which can be used for extraction of metals⁷ and natural products^{8,9}. In addition to this, in an attempt to reduce the viscosity associated with these charged DES species, Ribeiro *et al.* developed DES systems using D-menthol and carboxylic acid hydrogen bond donors where the individual components used are non-ionic species.¹⁰ More recently, DES made with the combination of trioctylphosphine oxide (TOPO) and phenol have been published and its use as a uranyl extractant shown.¹¹

TOPO has a number of uses such as capping agents¹²⁻¹⁶ in nanoparticle synthesis, metals^{17,18}, organic acids¹⁹⁻²² and phenolics²³⁻²⁶ extraction and so a number of DES will be prepared using a range of hydrogen bond donors most suited to the potential application.

Objective of this work

In this work, extraction of gallium from simulated waste zinc leach residue is carried out by extracting gallium from an acidic chloride aqueous phase. A 2:1 TOPO:malonic acid eutectic extractant is used to extract gallium up to 100% due to acting as a highly concentrated liquid extractant.

Progress to date

Following on from previous reports where a TOPO:Malonic acid eutectic in a 2:1 ratio was shown to extract gallium from an acidic chloride source with a LogD_{Ga} approximately 3 times greater than that

of the literature benchmark¹⁷ when conditions were replicated, competitive metal salt extraction focusing on PbCl_2 , ZnCl_2 , FeCl_3 , NaCl , CaCl_2 has been studied. These metal chloride salts have been chosen due to their presence as zinc leach residue from the zinc manufacturing process which would otherwise be dumped as waste.^{27–29}

Firstly, each metal salt was dissolved individually in a range of HCl concentrations from 1–8 M. PbCl_2 did not dissolve in HCl concentrations within the range studied and so extraction experiments were not carried out using PbCl_2 , however, all other metal chloride salts were dissolved in HCl individually and the extraction ability of 2:1 TOPO:malonic acid for each of these metal salts was studied. The results of this experimental study is shown in Figure 8 below.

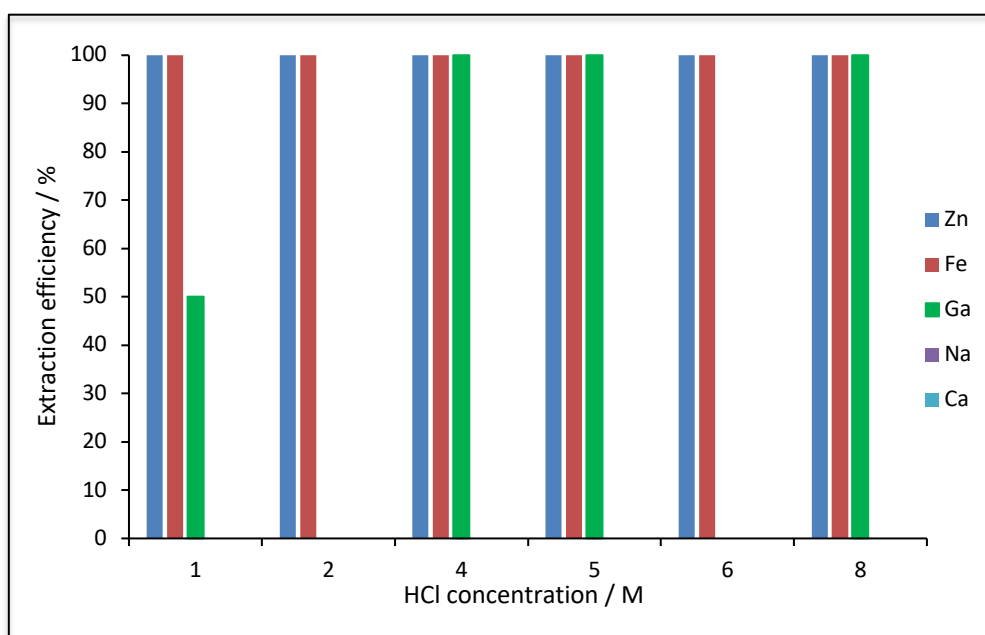


Figure 8. Extraction efficiency of metal chloride salts over a range of HCl concentrations using a 2:1 TOPO:malonic acid eutectic extractant. Org:aq 1:1, shaking time 10 mins, RT.

Figure 8 above shows that gallium extraction increases from 50–100% from 1–4 M HCl and remains at 100% above 4 M HCl thought to be due to an increased propensity to form tetrachlorogallate species with increasing HCl concentration to 8 M HCl. Competitive metal chloride salts also present in the zinc leach residue such as ZnCl_2 and FeCl_3 have extraction to the limits of detection (100%) across the whole HCl concentration range studied and so it is noted that in downstream recovery processes, the effect of these metal salts on gallium recovery will have to be considered. It is also evident, however, that NaCl and CaCl_2 are not extracted (0%) by 2:1 TOPO:malonic acid and so will not be present in the eutectic phase which will be treated for gallium recovery. In addition to these experiments considering individual metal salts, acidic chloride solutions of mixed metal salts will also be studied in the near future containing Ga, Zn and Fe in the proportions which they are present in zinc leach residue. This will be done to identify any changes in extraction behaviour within a mixed metal system and to determine the extent of extraction within this system.

Attempts to identify the parameters to recover gallium from the eutectic extractant using electrodeposition have been investigated and remain ongoing. To date, it has been found that recovery of gallium from low HCl concentrated systems is limited due to the non-ionic nature of the 2:1 TOPO:malonic acid eutectic system and hence the lack of conductivity that comes along with that. It was hypothesised that with the addition of metal salts to this eutectic mixture that



conductivity would increase to a point which would be sufficient for cyclic voltammetry and electrodeposition experiments, however, due to the low solubility of the metal salts in the eutectic without pre-contact with a strong HCl solution, conductivity remained low. The addition of $[N_{2222}][BF_4]$ as a supporting electrolyte to the eutectic did not appear to have an effect on the conductivity achieved, potentially due to its limited solubility in the eutectic. However, in systems where the extent of gallium extraction is higher (*i.e.* between 4-8 M HCl) conductivity is increased due to the greater extent of metal salt which can be dissolved into the eutectic and possible acid co-extraction which likely occurs; yielding a greater number of ionic species within the eutectic. Further investigation into this gallium recovery route is currently being pursued.

In addition to this, contribution to a book chapter reviewing hydrophobic DES and their applications has been recently worked on.

Conclusions and future work

To conclude, competitive metal salt extraction studies have highlighted that, in addition to gallium chloride, both iron and zinc chloride salts are competitively extracted to the limits of detection across the whole HCl concentration range when studied in extraction from aqueous acidic chloride sources individually, however, sodium and calcium chloride salts are not competitively extracted. Therefore, while awaiting the results from mixed metal studies, it can be seen that in post extraction processing to recover gallium, using electrodeposition for example, that the effects of zinc and iron chloride salts also must be considered in the design of these experiments.

Initial studies into recovering gallium from the eutectic extractant phase at low HCl concentrations has proven to be limited due to the low conductivity which arises from the non-ionic component nature of the eutectic combined with the low levels of metal chloride salt dissolution in these systems. The effect of the addition of a supporting electrolyte such as $[N_{2222}][BF_4]$ has also been limited due to its low solubility in the eutectic itself. However, more promising preliminary results have been achieved when attempting to increase conductivity by using the eutectic extractant phase after pre-contact with 6 M HCl thought to be due to acid co-extraction and the increased dissolution of metal chloride salts in the eutectic which increase the ionic nature of the extractant. This is promising as eutectic pre-contact is not an additional step in the recovery procedure, but instead is part of the initial extraction procedure itself. Greater gallium extraction efficiencies are also achieved at these HCl concentrations.

Initially, future work will involve extraction of gallium from a mixed metal system containing the metal chloride salts identified as competitive extractable species by the 2:1 TOPO:malonic acid eutectic in order to determine the effect that the relative abundance of each of these metal salts found in zinc leach residue will have on the extent of gallium extraction.

In addition to this, as co-extraction of iron and zinc chloride species is expected along with the extraction of gallium chloride species, as seen by the extraction of the individual metal salts, cyclic voltammetry will be performed with each of these metal salts past the point of their reduction to identify the voltage at which their electrodeposition would likely occur and if it would interfere with the electrodeposition of gallium if electrodeposition voltages overlapped for example or if the presence of water in the eutectic phase limits the electrochemical window of the eutectic phase. These studies will be performed with 2:1 TOPO malonic acid extractant phase first pre-contacted with 6 M HCl and with the concentration of each metal salt extracted added first individually and subsequently with mixed metal salts.

References

- (1) A. P. Abbott, G. Capper, D. L. Davies, H. L. Munro, R. K. Rasheed and V. Tambyrajah, *Chem. Commun.*, 2001, 2010–2011.
- (2) Q. Zhang, K. De Oliveira Vigier, S. Royer and F. Jérôme, *Chem. Soc. Rev.*, 2012, **41**, 7108.
- (3) M. Francisco, A. Van Den Bruinhorst and M. C. Kroon, *Angew. Chem. Int. Ed.*, 2013, **52**, 3074–3085.
- (4) E. L. Smith, A. P. Abbott and K. S. Ryder, *Chem. Rev.*, 2014, **114**, 11060–11082.
- (5) A. P. Abbott, D. Boothby, G. Capper, D. L. Davies and R. K. Rasheed, *J. Am. Chem. Soc.*, 2004, **126**, 9142–9147.
- (6) D. J. G. P. van Osch, L. F. Zubeir, A. van den Bruinhorst, M. A. A. Rocha and M. C. Kroon, *Green Chem.*, 2015, **17**, 4518–4521.
- (7) D. J. G. P. van Osch, D. Parmentier, C. H. J. T. Dietz, A. van den Bruinhorst, R. Tuinier and M. C. Kroon, *Chem. Commun.*, 2016, **52**, 11987–11990.
- (8) J. Cao, M. Yang, F. Cao, J. Wang and E. Su, *ACS Sustain. Chem. Eng.*, 2017, **5**, 3270–3278.
- (9) J. . Cao, L. . Chen, M. . Li, F. . Cao, L. . Zhao and E. Su, *Green Chem.*, 2018, **20**, 1879–1886.
- (10) B. D. Ribeiro, C. Florindo, L. C. Iff, M. A. Z. Coelho and I. M. Marrucho, *ACS Sustain. Chem. Eng.*, 2015, **3**, 2469–2477.
- (11) M. Gilmore, E. N. Mccourt, F. Connolly, P. Nockemann and J. D. Holbrey, *ACS Sustain. Chem. Eng.*, 2018, **6**, 17323–17332.
- (12) I. Mekis, D. V Talapin, A. Kornowski, M. Haase and H. Weller, *J. Phys. Chem.*, 2003, **107**, 7454–7462.
- (13) F. V Mikulec, M. Kuno, M. Bennati, D. A. Hall, R. G. Griffin and M. G. Bawendi, *J. Am. Chem. Soc.*, 2000, **122**, 2532–2540.
- (14) T. Cassagneau, T. E. Mallouk and J. H. Fendler, *J. Am. Chem. Soc.*, 1998, **120**, 7848–7859.
- (15) T. Trindade and P. O. Brien, *Chem Mater*, 1997, **9**, 523–530.
- (16) A. A. Guzelian, J. E. B. Katari, A. V Kadavanich, U. Banin, K. Hamad, E. Juban, A. P. Alivisatos, R. H. Wolters, C. C. Arnold and J. R. Heath, *J. Phys. Chem.*, 1996, **100**, 7212–7219.
- (17) T. Sato, T. Nakamura and S. Ishikawa, *Solvent Extr. Ion Exch.*, 1984, **2**, 201–212.
- (18) E. K. Watson and W. A. Rickelton, *Solvent Extr. Ion Exch.*, 1992, **10**, 879–889.
- (19) P. O. . Saboe, L. P. . Manker, W. E. . Michener, D. J. . Peterson, D. G. . Brandner, S. P. . Deutch, M. . Kumar, R. M. . Cywar, B. G. T.; and E. M. Karp, *Green Chem.*, 2018, **20**, 1791–1804.
- (20) T. Brouwer, M. Blahusiak, K. Babic and B. Schuur, *Sep. Purif. Technol.*, 2017, **185**, 186–195.
- (21) G. Kim, S. Park and B. Um, *Ind. Crop. Prod.*, 2016, **89**, 34–44.
- (22) S. Uenoyama, T. Hano, M. Hirata and S. Miura, *J. Chem. Technol. Biotechnol.*, 1996, **67**, 260–264.
- (23) P. Praveen and K. C. Loh, *Chem. Eng. J.*, 2014, **255**, 641–649.
- (24) P. Praveen and K. Loh, *Chemosphere*, 2016, **153**, 405–413.
- (25) P. Praveen and K. Loh, *J. Memb. Sci.*, 2013, **437**, 1–6.
- (26) P. Taylor, E. K. Watson, W. A. Rickelton, A. J. Robertson and T. J. Brown, *Solvent Extr. Ion Exch.*, 1988, **6**, 207–220.
- (27) T. Kinoshita, Y. Ishigaki, N. Shibata, K. Yamaguchi, S. Akita, S. Kitagawa, H. Kondou and S. Nii, *Sep. Purif. Technol.*, 2011, **78**, 181–188.
- (28) F. Liu, Z. Liu, Y. Li, Z. Liu, Q. Li and L. Zeng, *Hydrometallurgy*, 2016, **164**, 313–320.
- (29) X. Wu, S. Wu, W. Qin, X. Ma, Y. Niu, S. Lai, C. Yang, F. Jiao and L. Ren, *Hydrometallurgy*, 2012, **113–114**, 195–199.



QUILL Quarterly Report

May 2019 – July 2019

Name:	Dr Martyn Earle		
Supervisor(s):			
Position:	Senior Research Fellow		
Start date:	01-09-2018	Anticipated end date:	31-12-2019
Funding body:	BBSRC		

Microemulsion Solvent Systems for Bio-Separations

Background

The separation of proteins and related compounds often involves the use of aqueous biphasic solvent systems for both solvent extraction and countercurrent chromatographic separation. In this work we have developed a methodology capable of performing the separation of a two-component mixture of two proteins, which uses water as the mobile phase. A new aqueous biphasic solvent system has been developed which can selectively dissolve proteins and has been successfully tested in a centrifugal partition chromatography apparatus using a water/ hydrophobic microemulsion solvent system.

Objective of this work

The objectives of the work are to develop a clean, high capacity methodology for separating peptides and proteins, using ionic liquid containing stationary phases and water as a mobile phase in countercurrent chromatography and centrifugal partition chromatography.

Progress to date

The work has developed and tested a model separation of lysozyme from cytochrome C in the CPC apparatus. The separation achieved a complete separation of the two proteins, and the research has led to the development of new water / hydrophobic microemulsion solvent systems.

Conclusions and future work

The separation of lysozyme from cytochrome C has been successfully tested and a suitable range of solvent systems designed for protein separations have been developed. The mobile phase being comprised of water (saturated with an organic solvent) contains very low levels of involatile ionic liquids, which can be solvent extracted and recycled from the aqueous solution of separated proteins emerging from the CPC apparatus. This results in the protein solution containing no other involatile materials which makes the isolation of the protein from water very simple. The future work is to optimise the lysozyme / cytochrome C separation, and test a wider range of separations.

Microemulsion Solvent Systems for Bio-Separations

Dr Martyn Earle

28-08-2019

Introduction

The manufacture of high-value pharmaceutical products (such as peptides and proteins) require fast, low cost, reliable, GMP-compliant, scalable preparatory chromatography processes and technologies. By the use of a combination of three relatively new technologies, namely: (1) ionic liquids,¹ (2) modern high performance countercurrent chromatography (HPCCC)² or centrifugal partition chromatography (CPC)³ and (3) co-solvent free, high water content microemulsions⁴ (Figure 1) derived from cationic surfactants (surface active hydrophobic ionic liquids),⁵⁻⁷ we propose their combined use in enabling a new range of high performance and environmentally friendly separations of proteins and peptides. The importance and motivation for this research is that ionic liquids have been found to be excellent solvents for proteins,¹⁰ and have been demonstrated to work in a highly effective manner in countercurrent chromatography (CCC).^{9,11} Taken together, this enables peptide and protein separations to be carried out at much higher concentrations and space time yields,¹² using relatively small amounts of solvent, than is currently possible with conventionally used solvent systems.¹³ Since CCC separations with ionic liquids and high water content microemulsions behave in a different manner, and have different selectivities, when compared to HPLC, gel or size exclusion chromatography, electrophoresis and other methodologies used in protein purification,^{14,15} it will complement currently available technologies.¹⁴

This research is based on the discovery of a new “revolutionary” triphasic solvent system (Figure 1) and new biphasic water / hydrophobic microemulsion solvent systems based on ethyl ethanoate.

These separations use the cheapest liquid solvent available (water) as a mobile phase and relatively cheap organic solvents such as hexane or ethyl ethanoate. The ionic liquid which has been tested is at most 1.5 mol% or 10 wt% of the stationary phase making separations economical when compared to aqueous biphasic solvent systems based of $K_2[HPO_4]$ / PEG or $K_2[HPO_4]$ / $[C_4mim]Cl$. These separations are generally tolerant of solids which would normally block or destroy a HPLC or gel chromatography column, making the CPC separations much more robust and insensitive to particulate matter often found in crude protein samples. The

water / ionic liquid + organic solvent microemulsion solvent systems used in CPC separations have solute capacities of **1 to 2 order of magnitude** higher than those used in HPLC, and since the stationary phase is a liquid, rather than a surface (as in solid HPLC columns), the stationary phase can have much higher solute capacities than is found in similarly sized HPLC columns.¹⁹ Thus, far lower quantities of solvent per gram of protein are required in CPC separations, than is the case for HPLC separations.¹⁹ These ionic liquid and microemulsion solvent systems, combined with automated CPC apparatus and technologies have the potential to revolutionise the way in which proteins, enzymes and biopolymers are produced and dramatically reduce the production costs.



Figure 1 - An triphasic solvent system made from a mixture of water, hexane and a cationic surfactant (Fig 2.) The middle microemulsion phase is 75 mol% water. The lower phase is 99.7 mol% water and 0.3 mol% hexane, and the upper phase is excess hexane.^{6,7} The high-water content microemulsion (middle phase) is remarkable in that it requires no co-solvents and is termed “hydrophobic water”.

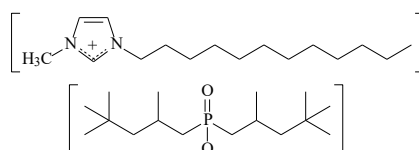


Figure 2 - The structure of the microemulsion forming ionic liquid $[C_{12}mim][DiIOP]$, which is used to form the “hydrophobic water phase” in Figure 1.

In liquid-liquid chromatography (LLC, HPLCC and CPC), a solute or analyte is partitioned between two liquid phases, where one phase is a mobile phase (MP) and one phase is a stationary phase (SP) (Fig. 3). The distribution ratio (K_D) of a solute between the two phases where $K_D = [\text{Solute}]_{\text{SP}}/[\text{Solute}]_{\text{MP}}$ determines the elution rate of the solute. Thus, in LLC, biphasic solvent systems are chosen or designed that give values of K_D in the 0.5 to 3.0 range. For many bio-molecules which are water soluble, aqueous biphasic solvent (ABS) systems are commonly used, which are comprised of two immiscible water containing phases. These usually contain polymers (such as polyethylene glycol or PEG) and concentrated inorganic salt solutions and are shaded in light grey (Table 1). More recently, an ionic liquid / concentrated inorganic salt solvent system (medium grey in Table 1) has been tested in LLC, and has higher solute capacities than PEG solvent systems.²⁰⁻

22

Table 1 A comparison of four aqueous biphasic solvent systems^{7,23-26}

Aqueous biphasic solvent system	Stationary Phase Composition (mol%)	Mobile Phase
Water – Hexane – [C₁₂mim][DiIOP] (Fig. 1)	Water 75%, Hexane 23.5%, [C₁₂mim][DiIOP] 1.5%	Water
Water-PEG-K ₂ [HPO ₄]	Water-polyethylene glycol	Water - K ₂ [HPO ₄]
[C ₄ mim]Cl-2.5M K ₂ [HPO ₄]-Water	87% water, 13% [C ₄ mim]Cl	Water – 4M K ₂ [HPO ₄]
Water - PEG - Dextran	Water - Dextran	Water - PEG

PEG = polyethylene glycol, [C₄mim]Cl = 1-butyl-3-methylimidazolium chloride, [C₁₂mim][DiIOP] = 1-dodecyl-3-methylimidazolium diisooctylphosphinate (or di(2,4,4-trimethylpentyl)phosphinate).

Experimental

Phase retention Curves

A biphasic solvent system was made by mixing water (2000 ml), ethyl ethanoate (1000 ml). To mixture 950 ml of water saturated ethyl ethanoate phase and 1000ml water saturated with ethyl ethanoate phase (MP) in a 3000 ml beaker, 1-decyl-3-methylimidazolium di-(2,4,4-trimethylpentyl)-phosphinate [C₁₀mim][DiIOP] (50.0 g) was added to make an approximately 5% solution of [C₁₀mim][DiIOP] dissolved in 950 ml of ethyl ethanoate. The NMR spectra of this solvent system (upper stationary phase (SP) and lower mobile phase (MP) was recorded to determine the composition of this biphasic mixture. The AECS/ECOM CPC instrument (Figures 3 and 4) was washed out with ethanol and all pumps and the instrument were filled with mobile phase, to displace the ethanol. The solvent reservoir was filled with 1 litre of MP and 1 litre of SP, and the Pump 2 was filled with SP from the top of the solvent reservoir. The instrument was filled with stationary phase through Pump 2, and the displaced mobile phase was returned to the solvent reservoir *via* the return pipe (Spider valve position = B1, VICI flow direction valve set to Position B to make the least dense phase become the stationary phase) with the rotation rate set to 400 RPM. When the instrument was full of SP, Pump 2 was stopped. The stationary phase retention curve for 5 wt% [C₁₀mim][DiIOP] + ethyl ethanoate / water solvent system was performed as follows:

- The level of the phase boundary was recorded at start of experiment.
- Spider valve position set to A1, and the VICI valve was set to position B
- Pump 1 set to flow rates increasing in the following order 3.0, 4.0, 5.0, 7.0, 8.5, 10.0, 12, 15, 20, 25, 30, 35, 40 ml/min.
- For each flow rate, take reading of the MP / SP level (the SP/MP phase boundary) in the solvent reservoir after the level in the solvent reservoir had reached a stable level, and have only mobile phase passing through the detector (no sharp peaks in the UV-Vis detector output due to stationary phase passing through the detector).

- (e) For each flow rate, measure the pressure reading on the pump pressure sensor.
- (f) For each flow rate, calculate the % stationary phase retention value (SPR) in the CPC rotor, using a value of 12 cm³ for the dead volume (DV - the internal volume of the pipes, detector, valves etc.) and 900 cm³ for the internal volume or capacity of the rotor (RC). % SPR = 100 x (IL-L-DV)/RC.
- (g) Figures 5 and 6 shows the SPR graphs of the 5% [C₁₀mim][DiIOP] + ethyl ethanoate / water solvent system at 400 RPM and 30 C.

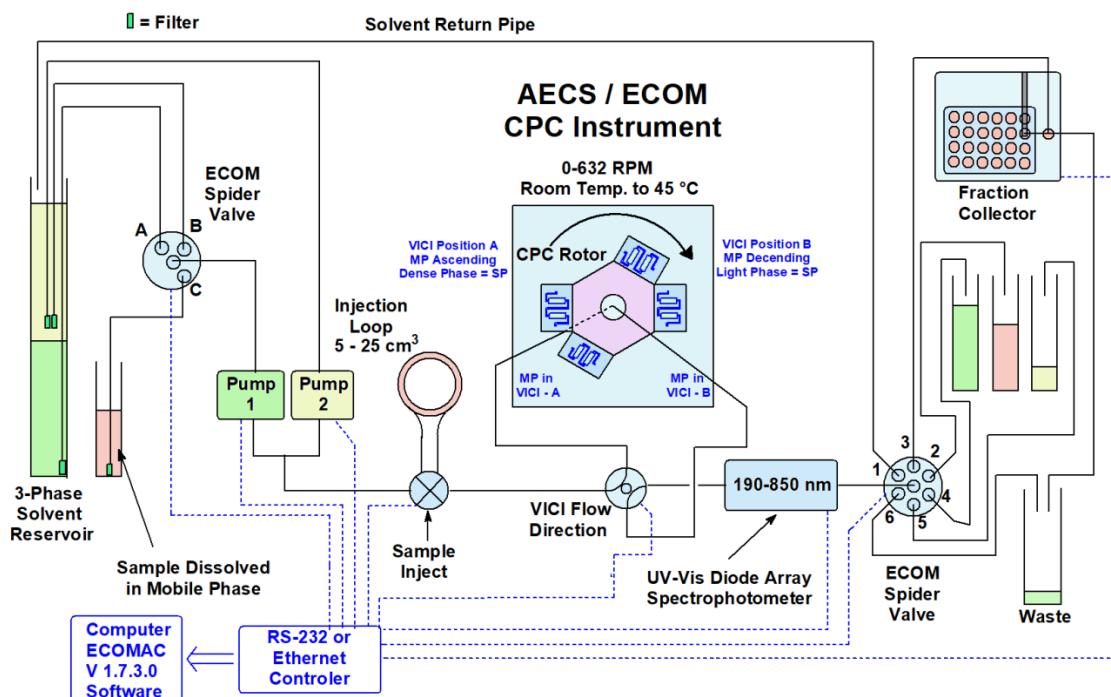


Figure 3 - The full schematic of the full AECS / ECOM CPC instrument in laboratory 02.201. The instrument is set up to use biphasic solvent systems and can use UV-Vis spectrometer to control the Spider and VICI valves, and pumps allowing collection of samples with specific absorption peaks or spectra. The computer control of the detector, pumps, valves and fraction collector allows fully automated separations.

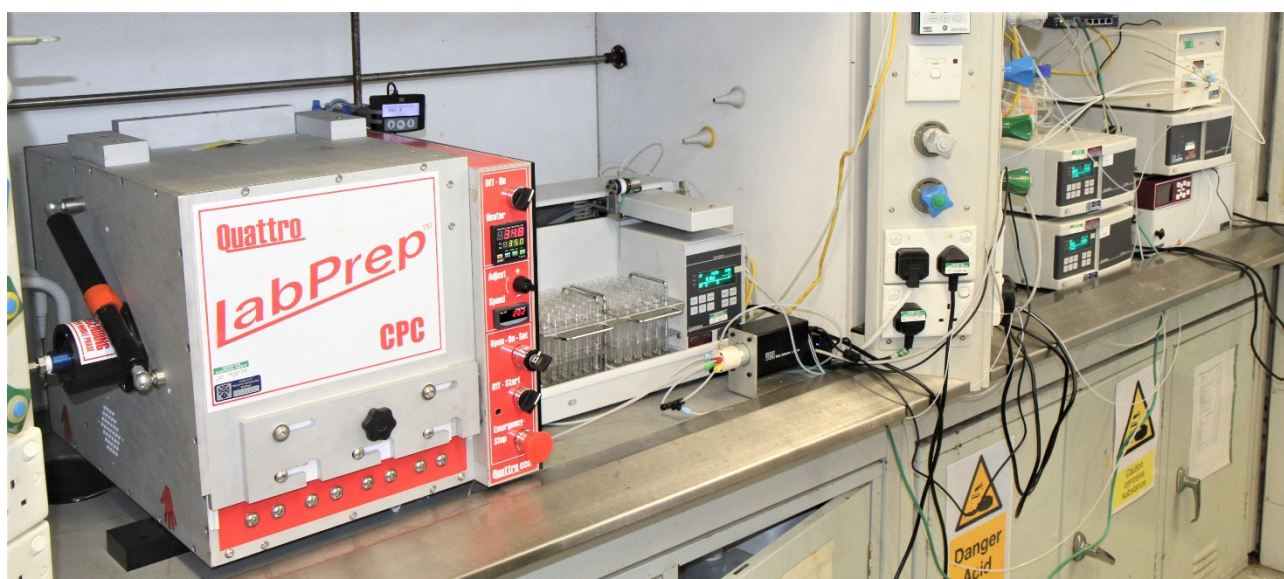


Figure 4 - The AECS centrifugal partition chromatography (CPC) machine installed in the QUILL Laboratories.

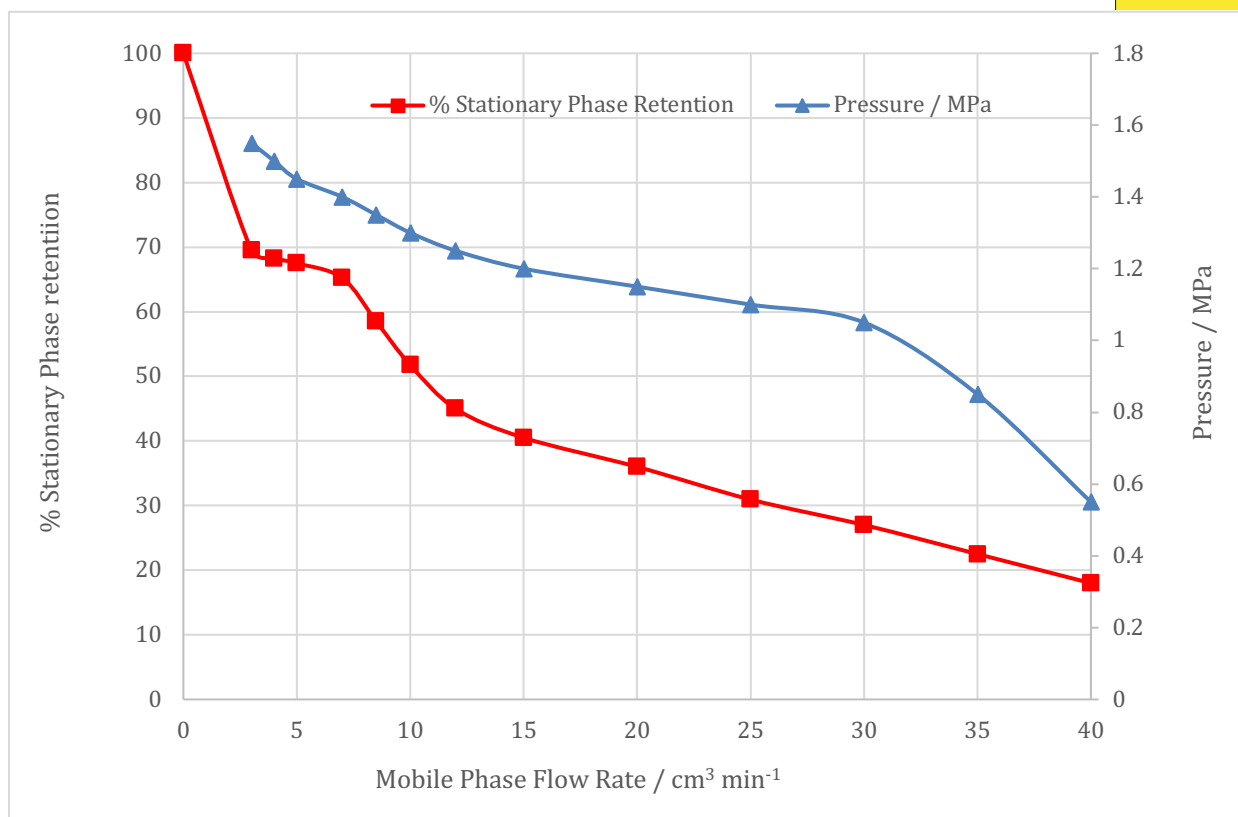


Figure 5 - The % stationary phase retention curve and pressure for the water / ethyl ethanoate + 5.0 wt% $[\text{C}_{10}\text{mim}][\text{DiIOP}]$ at 400 RPM and 30 °C, with ethyl ethanoate saturated water as the mobile phase.

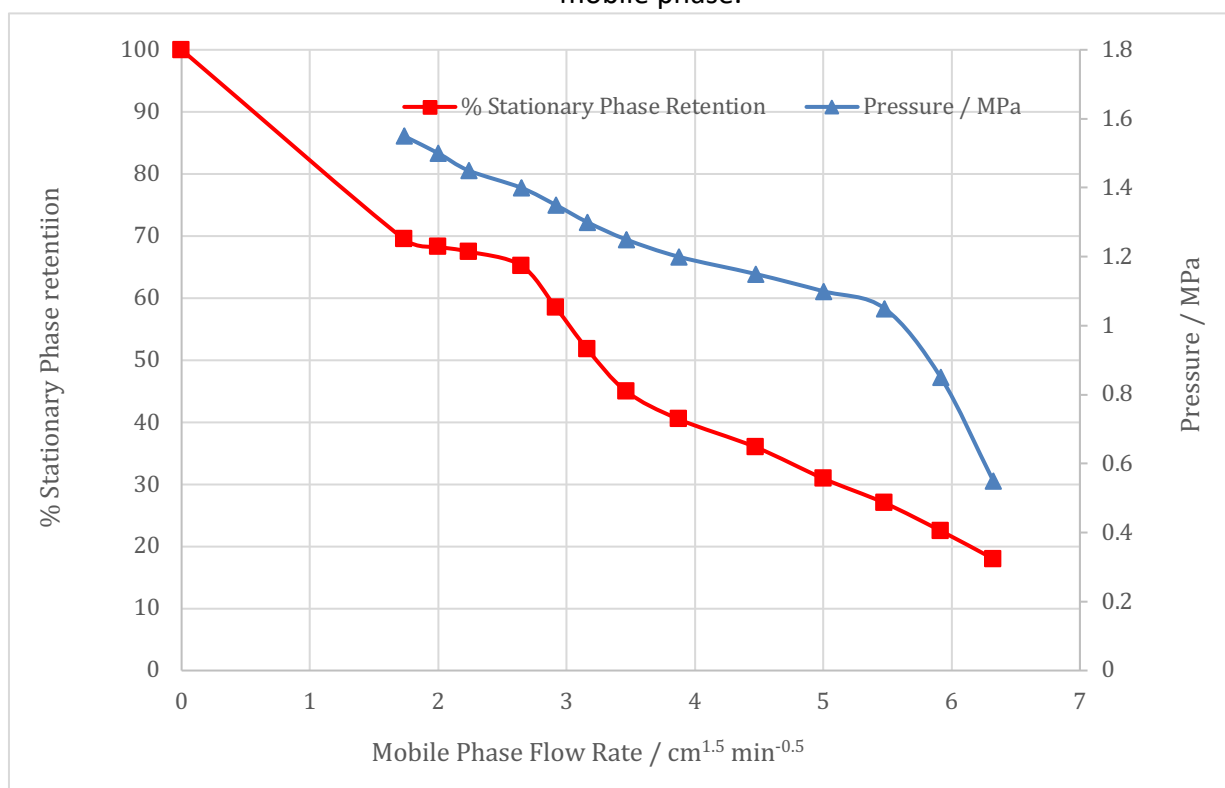


Figure 6 - The % stationary phase retention and pressure vs the square root of the flow rate for the water / ethyl ethanoate + 5.0 wt% $[\text{C}_{10}\text{mim}][\text{DiIOP}]$ at 400 RPM and 30 °C, with water as the mobile phase.



The stationary phase retention curves and corresponding CPC inlet pressure are shown in Figures 5 and 6. The deviation from ideal behaviour at 3-10 cm³ min⁻¹ flow rates is thought to be due to wetting effects of the microemulsion phase in the CPC rotor. Otherwise, the stationary phase retention (SPR) is proportional to the square root of the flow rate (Figure 6). The optimal flow rate for separations (where the gradient of the SPR curve is the lowest) with this solvent system is in the range of 3.0-7.0 cm³ min⁻¹.

Protein separations

A model protein separation of lysozyme / cytochrome C was tested to determine whether microemulsion solvent systems can be used in separations using CPC instrument shown in Figures 6 and 7. The solvent system chosen was a water / ethyl ethanoate solvent system containing the ionic liquid [C₁₀mim][DiIOP].

The distribution ratio of lysozyme between water and ethyl ethanoate containing [C₁₀mim][DiIOP] was measured by UV-Vis spectroscopy. A biphasic solution containing water and ethyl ethanoate was prepared and 10 cm³ of each phase of this solvent system were placed in a 40 cm³ centrifuge tube. 25 mg of lysozyme was added and the mixture shaken until the lysozyme dissolved. The tube was placed in a centrifuge and spun at 4400 RPM for 10 minutes, to allow both phases to become clear. The UV-Vis spectrum of both phases was recorded from 190-1100 nm using a 1.00 cm path length quartz UV-Vis cell. The absorption at 280 nm for lysozyme relative to the background at 350 nm was used to measure the concentration of lysozyme in each in each phase. The distribution ratio of lysozyme was then determined by dividing the absorbance of lysozyme in the stationary (ethyl ethanoate) phase by the absorption of lysozyme dissolved in the aqueous mobile phase. Increasing amounts of [C₁₀mim][DiIOP] was added to the mixture in the centrifuge tube, and the absorptions at 280 nm were determined for both phases, and the variation of distribution ratio was calculated and plotted graphically in Figure 7.

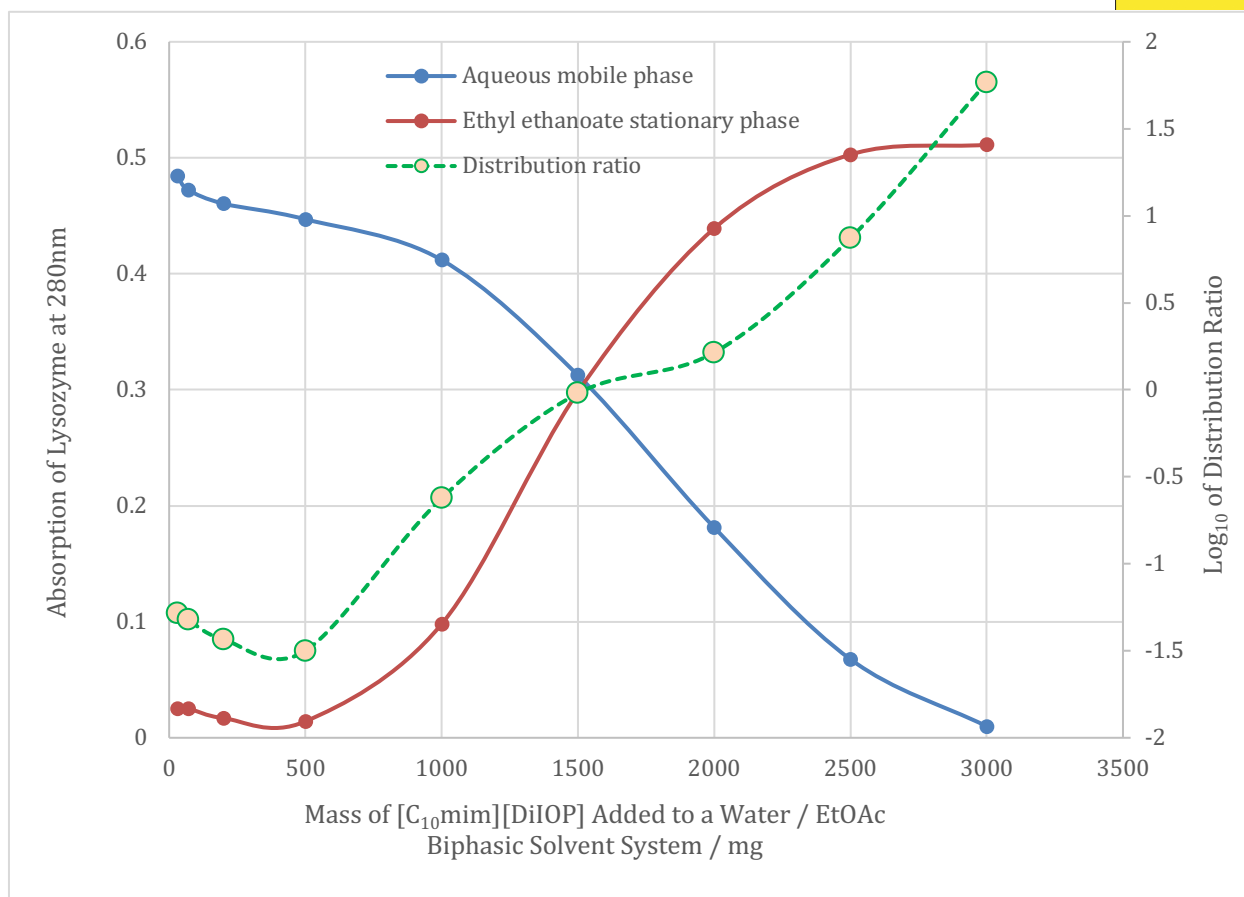


Figure 7 - Variation in the absorbance of lysozyme (25 mg) dissolved in a biphasic water / ethyl ethanoate solvent system consisting of 10 cm³ of each phase with the mass of [C₁₀mim][DiIOP] added to the ethyl ethanoate phase. The absorbance values are the absorbance of lysozyme at 280 nm – the background absorbance at 350 nm. The distribution ratio was calculated by dividing the lysozyme absorbance in the stationary phase with the absorbance of lysozyme in the mobile (water) phase.

The composition of the solvent system water / ethyl ethanoate + [C₁₀mim][DiIOP] was measured by adding known weights of [C₁₀mim][DiIOP] to a mixture of 15.0 cm³ of water saturated ethyl ethanoate and 15.0 cm³ of ethyl ethanoate saturated water in a centrifuge tube. After each addition of [C₁₀mim][DiIOP], the tube was centrifuged at 4400 RPM for 10 minutes and the ¹H NMR spectrum of both phases was measured in CD₃OD. The composition of the water / Ethyl Ethanoate + [C₁₀mim][DiIOP] solvent system is shown in Figure 8.

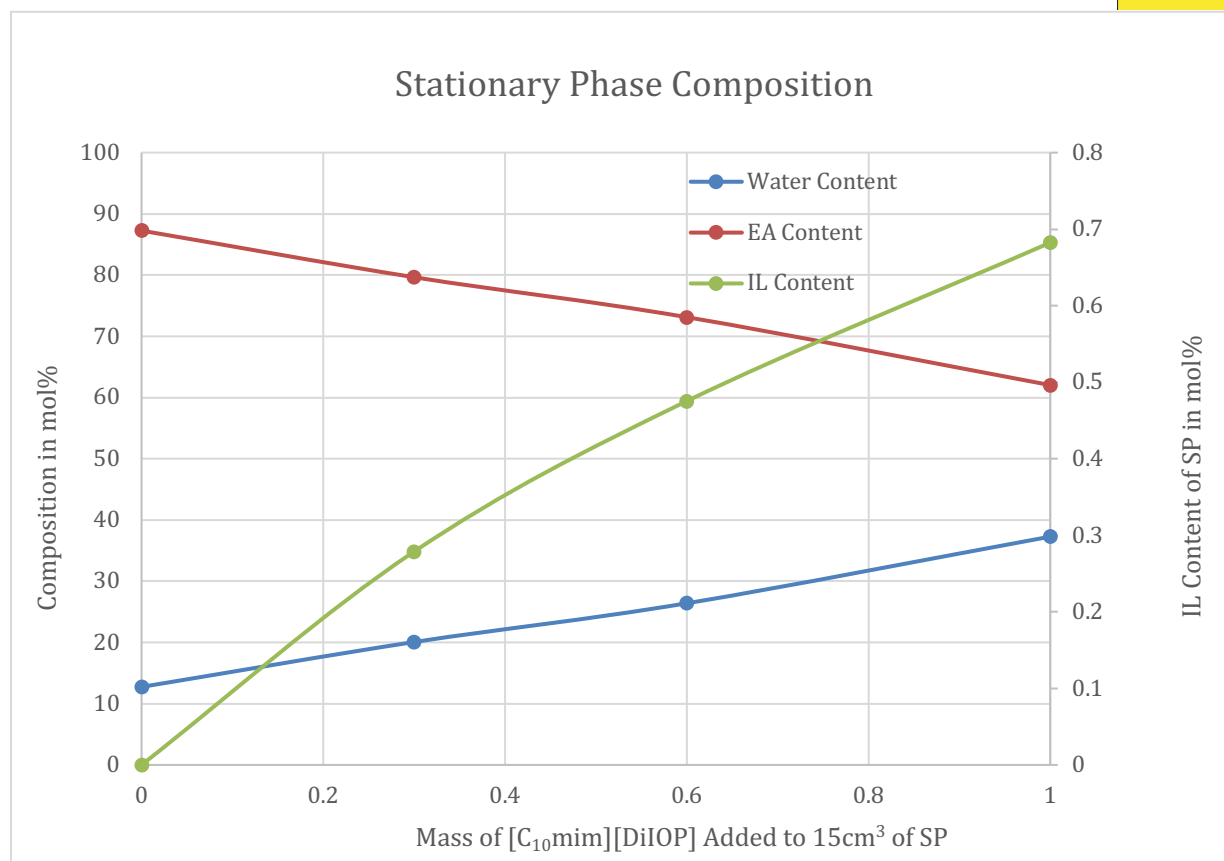


Figure 8. The composition of the stationary phase (15 cm^3 of the upper ethyl ethanoate phase) plotted against mass of $[C_{10}mim][DiIOP]$ added to the mixture of 15 cm^3 MP + 15 cm^3 SP.

The graph (Figure 8) shows that the ionic liquid $[C_{10}mim][DiIOP]$ causes water to dissolve in the hydrophobic ethyl ethanoate phase, and generated an aqueous biphasic solvent system, the composition of which, and the water content of the stationary phase can be controlled by the amount of ionic liquid added.

Separation Procedure

A biphasic mixture of water (2000 cm^3) and ethyl ethanoate (1200 cm^3) was prepared and the layers were separated. 2000 cm^3 of the aqueous phase and 950 cm^3 of the ethyl ethanoate phase were combined and 50 g $[C_{10}mim][DiIOP]$ was added, to form the water / $5\text{ wt}\%$ $[C_{10}mim][DiIOP]$ + ethyl ethanoate solvent system. The $10\text{ wt}\%$ $[C_{10}mim][DiIOP]$ solvent system was prepared from 2000 cm^3 of the above water phase, 900 cm^3 of ethyl ethanoate phase and 100 g of $[C_{10}mim][DiIOP]$. The CPC machine was filled with the stationary phase (ethyl ethanoate + $5\text{ wt}\%$ or $10\text{ wt}\%$ $[C_{10}mim][DiIOP]$). The rotation rate was set to 400 RPM (5% phase) or 450 RPM (10% phase) at $30\text{ }^\circ\text{C}$ (5% phase) or $40\text{ }^\circ\text{C}$ (10% phase). The mobile phase (water saturated with ethyl ethanoate) was pumped into the CPC machine at $8.0\text{ cm}^3\text{ min}^{-1}$ (spider valve = position A1 and VICI valve = position B). For 4 hours until the reading on the detector had stabilised. A solution of 0.50 g lysozyme and 0.020 g cytochrome C was in 40 cm^3 of mobile phase was prepared and loaded into the container for Spider valve position C. The MP flow rate was reduced to $5.0\text{ cm}^3\text{ min}^{-1}$ and 20 cm^3 of sample was loaded into the CPC machine (spider valve = position C1, for 4.0 minutes), then the spider valve was set to position A1 for 100 minutes. The separated cytochrome C fraction was collected from 100-130 minutes (spider valve = position A4), and the lysozyme was collected from 130-200 minutes (spider valve = position A2). The separation was stopper after 250 minutes. The chromatogram is shown in Figure 12.

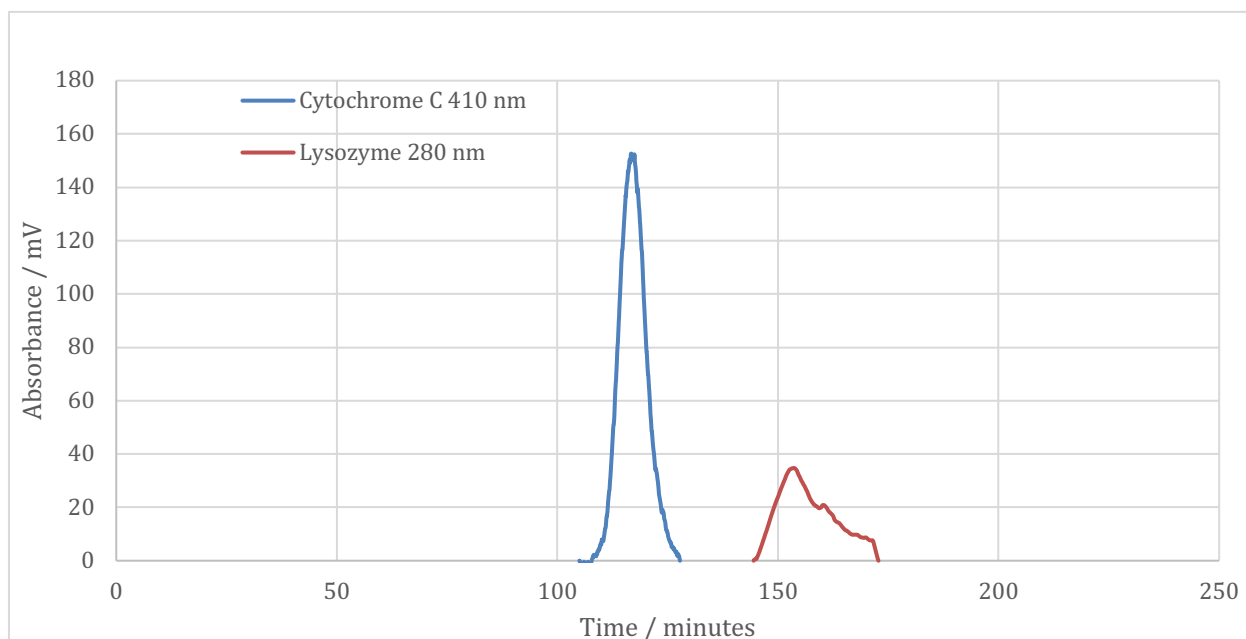


Figure 9. The chromatogram of 0.0125 g of Cytochrome C (410 nm) and 0.20 g of lysozyme (280 nm) using a 10.0 wt% [C₁₀mim][DiIOP] dissolved in water saturated ethyl ethanoate (900 cm³, stationary phase) and of ethyl ethanoate saturated water (2000 cm³, mobile phase) solvent system. The chromatogram was run at 450 RPM and 40 °C with cytochrome C measured at 410 nm and lysozyme measured at 280nm, with a baseline recorded at 350 nm.

Two separations were performed using the 5 wt% and 10 wt% [C₁₀mim][DiIOP] containing mixtures of water and ethyl ethanoate, with water as the mobile phase and ethyl ethanoate / [C₁₀mim][DiIOP] as the stationary phase. For the 5% [C₁₀mim][DiIOP] solvent system, only a partial separation was obtained, but with the 10% [C₁₀mim][DiIOP] solvent system, a complete protein separation occurred. The 10 wt% [C₁₀mim][DiIOP] separation is shown in Figure 9. This provides a proof of concept that protein separations are feasible using water / microemulsion solvent systems.

References

- (1) M. Freemantle, *An Introduction to Ionic Liquids*, The Royal Society of Chemistry, 2009.
- (2) A. Berthod and B. Billardello, *Advances in Chromatography*, Vol 40, 2000, **40**, 503-538.
- (3) A. Foucault and K. Nakanishi, *J. Liq. Chromatogr.*, 1990, **13**, 2421-2440.
- (4) H. Watarai, *J. Chromatogr. A*, 1997, **780**, 93-102.
- (5) M. Blesic, M. Swadzba-Kwasny, J. D. Holbrey, J. N. C. Lopes, K. R. Seddon and L. P. N. Rebelo, *Phys. Chem. Chem. Phys.*, 2009, **11**, 4260-4268.
- (6) I. R. Collins, M. J. Earle, S. P. Exton, N. V. Plechkova and K. R. Seddon, *World Pat.*, WO2006111712A2, 2006.
- (7) M. Hejazifar, M. Earle, K. R. Seddon, S. Weber, R. Zirbs and K. Bica, *J. Org. Chem.*, 2016, **81**, 12332-12339.
- (8) S. Y. Huang, Y. Z. Wang, Y. G. Zhou, L. Li, Q. Zeng and X. Q. Ding, *Anal. Methods*, 2013, **5**, 3395-3402.
- (9) L. Brown, M. J. Earle, M. A. Gilea, N. V. Plechkova and K. R. Seddon, *Aust. J. Chem.*, 2017, **70**, 923-932.
- (10) C. Schroder, *Top. Curr. Chem.*, 2017, **375**, 26.
- (11) L. Brown, M. J. Earle, M. A. Gilea, N. V. Plechkova and K. R. Seddon, *Top. Curr. Chem.*, 2017, **74**, 1-41.



- (12) G. W. Zheng, X. Y. Liu, Z. J. Zhang, P. Tian, G. Q. Lin and J. H. Xu, *RSC Adv.*, 2013, **3**, 20446-20449.
- (13) Y. H. Guan, P. Hewitson, R. van den Heuvel, Y. Zhao, R. P. G. Siebers, Y. P. Zhuang and I. Sutherland, *J. Chromatogr. A*, 2015, **1424**, 102-110.
- (14) H. Rehm, *Protein Biochemistry and Proteomics*, Academic Press, Elsevier Inc., Burlington, MA 01803, USA, 2006.
- (15) A. Rizwan, *Protein Purification*, InTech, Rijeka, Croatia, 2012.
- (16) A. A. Tietze, P. Heimer, A. Stark and D. Imhof, *Molecules*, 2012, **17**, 4158-4185.
- (17) Y. Ito and R. Clary, *Separations*, 2016, **3**, 7.
- (18) K. He, Z. Y. Zou, Y. R. Hu, Y. Yang, Y. B. Xiao, P. C. Gao, X. G. Li and X. L. Ye, *J. Sep. Sci.*, 2016, **39**, 703-708.
- (19) K. Faure, E. Bouju, P. Suchet and A. Berthod, *Anal. Chem.*, 2013, **85**, 4644-4650.
- (20) M. J. Ruiz-Ángel, V. Pino, S. Carda-Broch and A. Berthod, *J. Chromatogr. A*, 2007, **1151**, 65-73.
- (21) Z. G. Jiang, Q. Z. Du and L. Y. Sheng, *Chin. J. Anal. Chem.*, 2009, **37**, 412-416.
- (22) M. J. Earle and M. A. Gilea, *World Pat.*, WO2013140185A1, 2013.
- (23) I. R. Collins, M. J. Earle, S. P. Exton, N. V. Plechkova and K. R. Seddon, WO 2006111712 A2, 2006.
- (24) M. G. Freire, A. F. M. Claudio, J. M. M. Araujo, J. A. P. Coutinho, I. M. Marrucho, J. N. C. Lopes and L. P. N. Rebelo, *Chem. Soc. Rev.*, 2012, **41**, 4966-4995.
- (25) R. D. Rogers, A. H. Bond, C. B. Bauer, Y. Song, J. H. Zhang and R. R. Chomko, *Abstr. Pap. Am. Chem. Soc.*, 1994, **208**, 17-IEC.
- (26) M. L. Moody, H. D. Willauer, S. T. Griffin, J. G. Huddleston and R. D. Rogers, *Ind. Eng. Chem. Res.*, 2005, **44**, 3749-3760.
- (27) V. Singh, S. Panda, H. Kaur, P. K. Banipal, R. L. Gardas and T. S. Banipal, *Fluid Phase Equilib.*, 2016, **421**, 24-32.
- (28) J. M. Padro, A. Ponzinibbio, L. B. A. Mesa and M. Reta, *Anal. Bioanal. Chem.*, 2011, **399**, 2807-2820.
- (29) H. Miyafuji, *J. Wood Sci.*, 2015, **61**, 343-350.
- (30) S. Hina, Y. M. Zhang and H. P. Wang, *Rev. Adv. Mater. Sci.*, 2015, **40**, 215-226.
- (31) H. Garcia, R. Ferreira, M. Petkovic, J. L. Ferguson, M. C. Leitao, H. Q. N. Gunaratne, K. R. Seddon, L. P. N. Rebelo and C. S. Pereira, *Green Chem.*, 2010, **12**, 367-369.
- (32) M. Isik, H. Sardon and D. Mecerreyes, *Int. J. Mol. Sci.*, 2014, **15**, 11922-11940.
- (33) V. C. A. Orr, N. V. Plechkova, K. R. Seddon and L. Rehmman, *ACS Sustain. Chem. Eng.*, 2016, **4**, 591-600.
- (34) <http://www.grandviewresearch.com/industry-analysis/protein-purification-isolation-market>
- (35) K. Wilson and J. Walker, *Principles and techniques of biochemistry and molecular biology*, Cambridge University Press, Cambridge, UK, 6th edn., 2005.
- (36) Q. L. Luo, J. D. Andrade and K. D. Caldwell, *J. Chromatogr. A*, 1998, **816**, 97-105.
- (37) S. S. M. Noor, B. T. Tey, W. S. Tan, T. C. Ling, R. N. Ramanan and C. W. Ooi, *J. Liq. Chromatogr. Relat. Technol.*, 2014, **37**, 1873-1884.
- (38) Y. Ito, T. Mitani, N. Harada, A. Isayama, S. Tanimori, S. Takenaka, Y. Nakano, H. Inui and R. Yamaji, *Journal of Nutritional Science and Vitaminology*, 2013, **59**, 358-364.
- (39) D. Abd El-Hady, H. M. Albishri and R. Rengarajan, *Biomed. Chromatogr.*, 2015, **29**, 925-934.
- (40) D. A. El-Hady, H. M. Albishri, R. Rengarajan, S. El Deeb and H. Watzig, *Electrophoresis*, 2015, **36**, 3080-3087.
- (41) F. Hasan, P. Vidanapathirana, S. Das, V. E. Fernand, N. Siraj, J. N. Losso and I. M. Warner, *RSC Adv.*, 2015, **5**, 69229-69237.

QUILL Quarterly Report

May 2019 – July 2019

Name:	David Greene		
Supervisor(s):	Leila Moura		
Position:	Studentship		
Start date:	10/06/19	Anticipated end date:	31/08/19
Funding body:	QUILL		

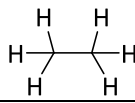
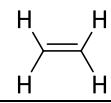
Gas Line Design for the NMR Study of Ethane and Ethylene Absorption

Background

The motivation for a greener and more sustainable method of gaseous separations for chemical companies is increasing, with the progression being aided by a societal, environmental and economical drive. Ethylene and propylene are some of the largest produced organic chemicals, showing it has a large global demand. Both ethylene and propene are precursors to produce a variety of products such as; fluorinated ethylene propylene (FEP) tubing, lubricants, prosthetics ⁽¹⁾ and is used for catalysis. ^(2,3)

The most common method for the separation of gaseous olefin/paraffin mixtures is cryogenic distillation. ⁽⁴⁾ It is used to separate chemicals with very low boiling points (e.g. propylene/propane mixture). However, as with its success, is the disadvantage of having a costly process due to the sheer size of the distillation columns, a large energy output ⁽⁵⁾ and environmental costs. ⁽⁷⁾ The environmental and economic problems arise due to the difficulty of separating olefin/paraffin samples where the physical properties are so close to one another, as listed in table 1. ⁽⁷⁾ The search for alternative separation processes led to the interest of using ionic liquids (ILs) as separating agents for olefin/paraffin gas separation.

Table 1 - Comparison of the properties of ethylene and ethane

	Ethane (C ₂ H ₆)	Ethylene (C ₂ H ₄)
Structure		
Hybridization	sp ³	sp ²
Molar mass / g mol ⁻¹	30.1	28.1
Melting Point / °C	-183	-169
Boiling Point / °C	-89.0	-104
Density / Kg m ⁻³	1.36	1.18
H-C-C Bond Angle / °	110	122
C-C bond length / pm	154	133
C-H bond length / pm	110	108



Objectives

The group's focus is to develop strategies for the separation of ethylene and propylene from their saturated counterparts using absorbents based in ionic liquids (ILs) and deep eutectic solvents (DES) rather than the energetically demanding cryogenic distillation used in industry. The assembly of a moderate pressure gas line will enable the safe use of gases such as ethylene and ethane to be manipulated using various techniques such as gas chromatography and phase equilibria studies, and moderate pressure proton NMR in particular to help identify the molecular structures involved in the absorption of ethane and ethylene.

Our goal is to determine if moderate pressure NMR can help in the determination of the critical molecular interactions involved in the absorption of ethane, ethylene, propane and propylene in ILs and DES.

Progress to date

During this studentship, I have looked into olefin/paraffin gas separations with ionic liquids using moderate pressure proton NMR ^(8,9) as well as other methods such as supported liquid membranes (SLMs) ^(10,11) and metal organic framework adsorbents (MOFs). ^(12,13) It has been reported that SLMs seem to not be suitable for scale up in industry due to their permeation performance deteriorating with evaporation of the liquid membrane and the MOFs studied ⁽¹³⁾ generally have a sensitivity to water, reducing their ability to adsorb targeted gases. Ionic liquids, however, present great potential and several advantages specific to gas separations due to their general low volatility and their "designer-solvent" properties.

From all the hydrocarbon gases, acetylene is the most commonly studied gas for targeted separation with ionic liquids using moderate pressure proton NMR. ^(14,15) For acetylene/ethylene mixtures, it was shown that more basic anions allowed for a greater solubility in acetylene. The reason for this was demonstrated by NMR, showing an enhanced acid-base interaction between the acidic proton of acetylene and a basic anion of the IL.

A well-designed gas line (Figure 1) is fundamental for the investigation of these gaseous olefin/paraffin separations. Specifically, this line was designed to assist in complex gas absorption studies through moderate pressure NMR, headspace gas chromatography and measurement of phase equilibria via a moderate pressure reactor.

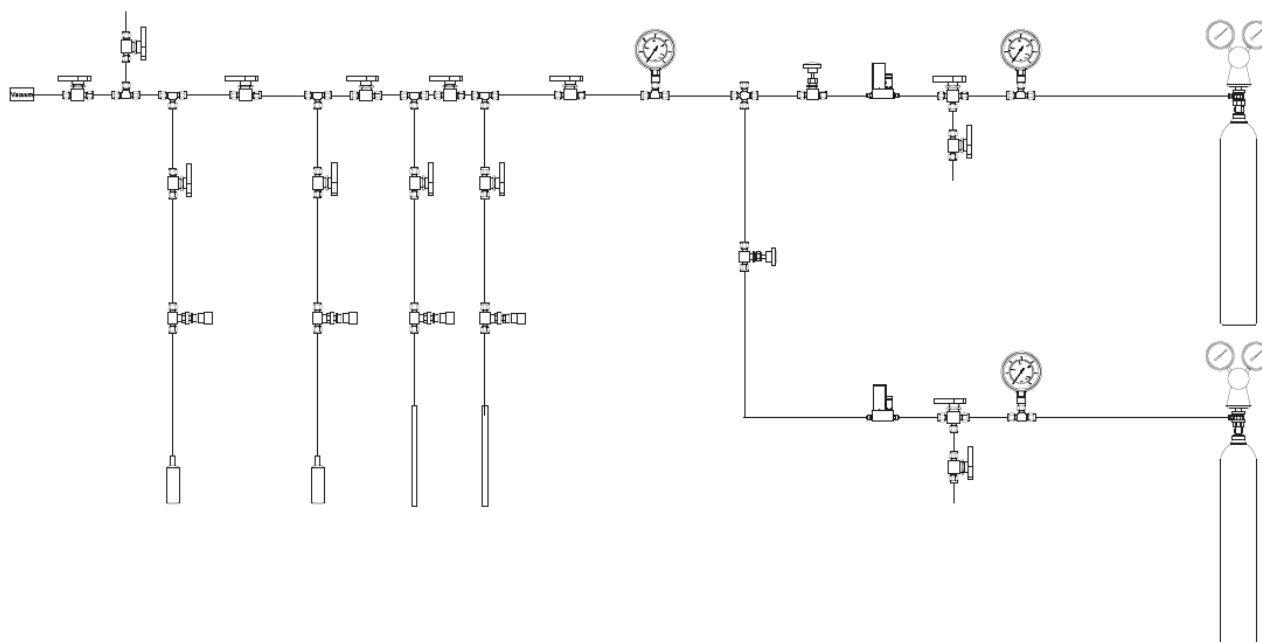


Figure 1 - Gas line designed for olefin/paraffin separation studies

Conclusions

Ionic liquids can be used as effective absorbents for hydrocarbon gaseous separations. The ability to tailor ILs to acquire specific properties is an advantage over using previously studied techniques such as SLMs and MOFs. Moderate pressure proton NMR has shown to be effective at identifying the molecular structures that are involved in the absorption of gaseous mixtures, particularly acetylene/ethylene. This opens up the opportunity to develop strategies for the separation of olefins such as ethylene and propylene from their saturated counterparts using absorbents based in ionic liquids and deep eutectic solvents.

Future work

Further work to be conducted is the extensive testing of the gas line and investigation of ethylene/ethane absorption using ionic liquids, analysed by moderate pressure proton NMR and gas chromatography.

References

- (1) W. J. Rogers, *Sterilisation techniques for polymers*, Elsevier Masson SAS., 2012.
- (2) T. Agapie, *Coord. Chem. Rev.*, 2011, **255**, 861–880.
- (3) W. Wang, H. Sun and C. Redshaw, *J. Organomet. Chem.*, 2014, 751, 717–741.
- (4) L. Li, R. B. Lin, R. Krishna, H. Li, S. Xiang, H. Wu, J. Li, W. Zhou and B. Chen, *Science*, 2018, 362, 443–446.
- (5) S. Mokhatab, W. A. Poe and J. Y. Mak, *Handb. Nat. Gas Transm. Process.*, 2018, 395–408.
- (6) M. Alhajji and Y. Demirel, *Int. J. Energy Environ. Eng.*, 2016, 7, 45–59.
- (7) Y. Sun, H. Bi, H. Dou, H. Yang, Z. Huang, B. Wang, R. Deng and L. Zhang, *Ind. Eng. Chem. Res.*, 2017, 56, 741–749.
- (8) F. Agel, F. Pitsch, F. F. Krull, P. Schulz, M. Wessling, T. Melin and P. Wasserscheid, *Phys. Chem. Chem. Phys.*, 2011, 13, 725–731.
- (9) S. Jung, J. Palgunadi, J. H. Kim, H. Lee, B. S. Ahn, M. Cheong and H. S. Kim, 2010, 354, 63–67.



- (10) S. Azizi, T. Kaghazchi and A. Kargari, *J. Taiwan Inst. Chem. Eng.*, 2015, 57, 1–8.
- (11) F. Pitsch, F. F. Krull, F. Agel, P. Schulz, P. Wasserscheid, T. Melin and M. Wessling, *Adv. Mater.*, 2012, **24**, 4306–4310. D
- (12) U. Bo, B. Barth, C. Paula, A. Kuhnt, W. Schwieger, A. Mundstock, J. Caro and M. Hartmann. *Langmuir*, 2013, 29, 8592–8600.
- (13) V. F. D. Martins, A. M. Ribeiro, A. Ferreira, U. H. Lee, Y. K. Hwang, J. S. Chang, J. M. Loureiro and A. E. Rodrigues, *Sep. Purif. Technol.*, 2015, 149, 445–456.
- (14) J. Palgunadi, H. S. Kim, J. M. Lee and S. Jung, *Chem. Eng. Process. Process Intensif.*, 2010, 49, 192–198.
- (15) J. M. Lee, J. Palgunadi, J. H. Kim, S. Jung, Y.-S. Choi, M. Cheong and H. S. Kim, *Phys. Chem. Chem. Phys.*, 2010, 12, 1812–1816.



QUILL Quarterly Report

May 2019 – July 2019

Name:	Anne McGrogan		
Supervisor(s):	Dr Gosia Swadźba-Kwaśny		
Position:	Summer studentship		
Start date:	03/06/19	Anticipated end date:	05/07/19
Funding body:	QUILL		

Encounter complexes in Frustrated Lewis Pairs

Background

Frustrated Lewis pairs (FLPs) are combinations of Lewis acids and Lewis bases which are sterically prevented from the formation of a typical Lewis acid-base adduct.¹ A typical example is the combination of tris(tert-butyl)phosphine ($P(tBu)_3$) as the Lewis base and tris(pentafluorophenyl)borane (BCF) as the Lewis acid. The phosphorus and boron centres in the two molecules provide highly catalytically active Lewis acidic and basic sites. The closeness of these reactive sites leads to remarkable reactivity, most notably in the activation of hydrogen and other small molecules.² This has led to the development of metal-free catalytic hydrogenations, which are extremely attractive due to the high cost, toxicity and sustainability of transition metals such as palladium and platinum.³

The H_2 activation by FLPs would be expected to follow trimolecular reaction kinetics as there are three species involved; the Lewis acid, Lewis base and H_2 . However, kinetic studies suggest that the reaction of an FLP solution with H_2 is bimolecular. This has given rise to the pre-organisational effect which is the idea that pre-arranged acid-base encounter complexes must be present in the solution.⁴

Conventional 1D NMR spectra of FLP solutions has failed to provide evidence for the encounter complex formation. However, previous work by the group demonstrated the presence of an encounter complex in a model FLP solution in benzene through neutron scattering studies and structure refinement with EPSR. The FLP used was $P(tBu)_3$ and BCF and the formation of the encounter complex confirmed using $P \cdots B$ correlation analysis. Approximately 5% of the dissolved FLP components remained associated to the encounter complex, in accordance with DFT results. The group then revealed how the population of encounter complexes of FLP can be enhanced using ionic liquids. The selected ionic liquid was 1-decyl-3-methylimidazolium bis(trifluoromethanesulfonyl)imide, $[C_{10}mim][NTf_2]$, which generated NMR signals of the FLP encounter complex consisting of over 20% of the dissolved components. These results indicate that ionic liquids can stabilise encounter complexes, resulting in a higher level of association and longer lifetime. This leads to greater catalytic activity in comparison to other traditional solvents like benzene. The FLP in the ionic liquid solution retained its ability to split hydrogen.⁵

Furthermore, previous work has shown that dissolving a sterically-hindered phosphine in ionic liquids with strongly Lewis acidic borenium cations are capable of H_2 splitting.

The work in June at the ISIS facility in Oxfordshire, using the instrument SANDALS (the Small Angle Neutron Diffractometer for Amorphous and Liquid Samples) investigated the interaction between Lewis



acidic and basic centres in the traditional FLP $P(tBu)_3/BCF$. Previous work by the group investigated the interaction of this FLP in the ionic liquid $[C_{10}mim][NTf_2]$.⁵ This time, the ionic liquid $[C_2mim][NTf_2]$ was used as it has a shorter chain length than $[C_{10}mim][NTf_2]$. This leads to lower viscosity and $[C_2mim][NTf_2]$ can be used in neutron scattering whereas the chain length in $[C_{10}mim][NTf_2]$ is too long to be used in neutron scattering as it can't be accurately modelled.

The work in July at the Diamond Light Source facility in Oxfordshire used P 1s and Cl 1s near-edge X-ray absorption fine structure (NEXAFS) spectroscopy with fluorescence detection to study a range of encounter complexes in solution. P 1s edge and Cl 1s edge NEXAFS spectroscopy are very effective methods for probing chemical bonding, in particular when electron transfer is involved, as is the case for Lewis acid-base interactions.

Objective of this work

The goal is for the work at ISIS to provide a crucial insight into the encounter complexes which form in FLP systems and potentially elucidate the reason for enhanced stability of FLP encounter complexes in ILs. Results from NEXAFS spectroscopy should help determine the nature of the interaction between the FLP components in various solvents. This will help to spectroscopically characterise the electronic structure of the encounter complexes. Furthermore, to understand, how the properties of the encounter complexes relate to FLP reactivity through a combination of experimental and computational results. This will aid the design of FLPs and optimisation of catalytic reactions.

Progress to date

I commenced the summer placement by preparing the samples for the upcoming trip to ISIS. The chemicals required were BCF, $P(tBu)_3$ and the ionic liquid $[C_2mim][NTf_2]$ which I synthesised. The deuteration lab at Diamond prepared the deuterated version of the ionic liquid. Table 1 shows the samples that were run at ISIS, highlighted in green. The other half of the samples will be run in October. The deuteration lab will prepare the deuterated phosphine.

	H- $P(tBu)_3$	BCF	H- $P(tBu)_3$ + BCF	D- $P(tBu)_3$	D- $P(tBu)_3$ + BCF	H & D- $P(tBu)_3$	H & D- $P(tBu)_3$ + BCF
H- $[C_2mim]$ $[NTf_2]$							
D- $[C_2mim]$ $[NTf_2]$							
H & D- $[C_2mim]$ $[NTf_2]$							

H = protonated D= deuterated

Table 1 -Samples for experiments at ISIS facility, highlighted in green are the samples that have been run.

After ISIS, a week was spent to prepare the samples for the experiments at Diamond. The samples that were run at Diamond are shown in Figure 1. The results from these samples will enable investigation into the nature of the interaction between the FLP components in various solvents. It will suggest how the properties of the encounter complexes relate to FLP reactivity which will aid the design of FLPs and optimise catalytic reactions.

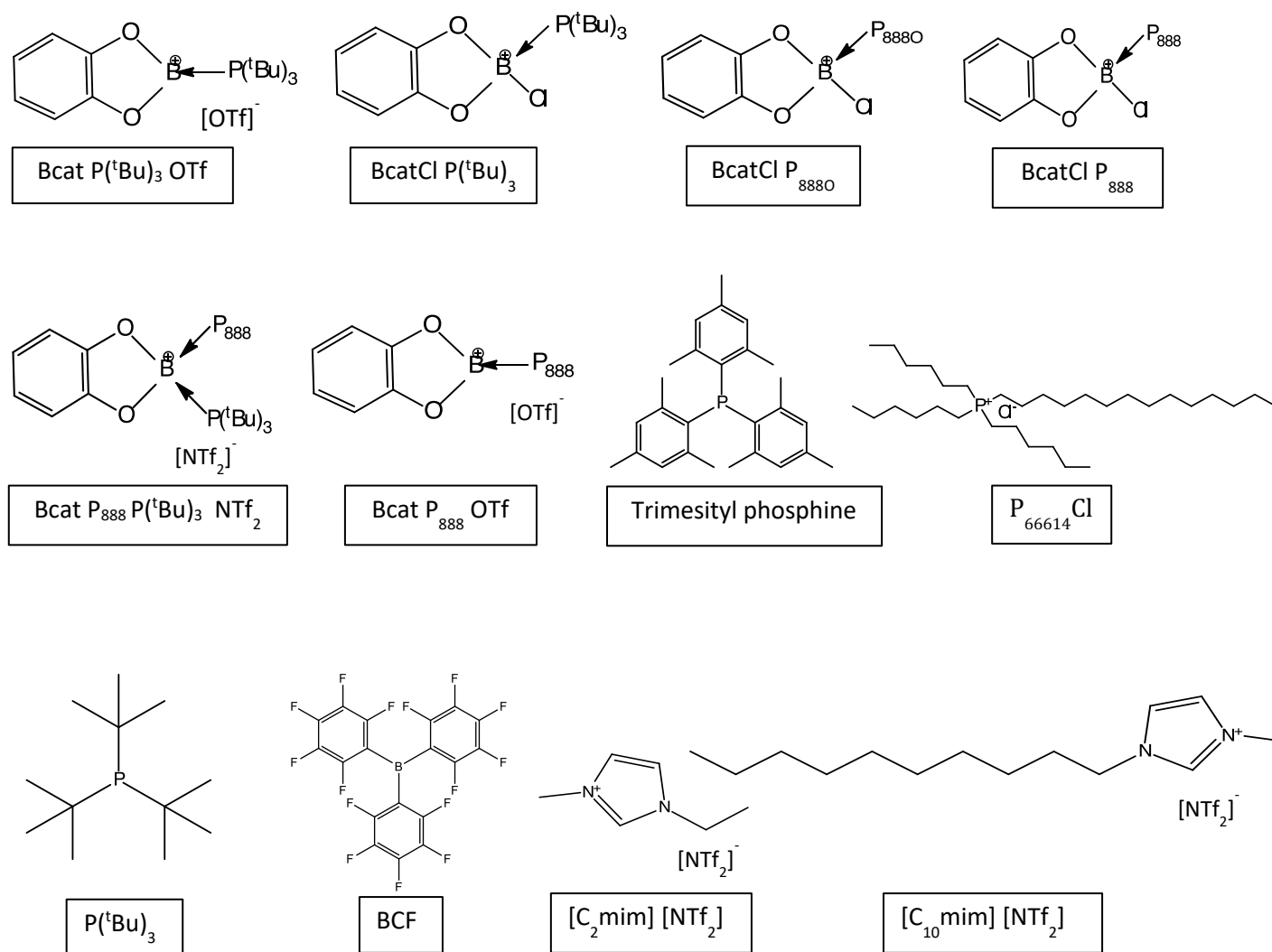


Figure 1: Samples run at Diamond Light Source.

Other samples prepared for Diamond were BcatCl, Bcat P_{888O} OTf and the ionic liquids $[C_2mim][FAP]$ and $[C_2mim][B(CN)_4]$.

Analysis of the results will be in collaboration with Dr. Kevin Lovelock at the University of Reading.

Conclusions and future work

In conclusion, the summer placement has involved preparing samples for the two trips to the ISIS facility and Diamond Light Source in Oxfordshire. Synthetic work was carried out before these trips to prepare the samples required. In October there will be a trip to ISIS to finish running the other half of the samples and then the results will be analysed. The results from the NEXAFS experiments in Diamond will be analysed in collaboration with Dr. Kevin Lovelock from the University of Reading.



Other future work involves investigating catalytic systems with known FLPs from literature to test their ability to activate hydrogen. The goal would be to apply these catalytic systems to supported ionic liquid phase (SILP) catalysis.

References

- (1) G. C. Welch, R. R. S. Juan, J. D. Masuda and D. W. Stephan, *Science* (80-.), 2006, **314**, S1–S11.
- (2) L. C. Wilkins, B. A. R. Günther, M. Walther, J. R. Lawson, T. Wirth and R. L. Melen, *Angew. Chemie - Int. Ed.*, 2016, **55**, 11292–11295.
- (3) J. R. Ludwig, C. S. Schindler and J. R. Ludwig, *CHEMPR*, 2017, **2**, 313–316.
- (4) T. A. Rokob, A. Hamza, A. Stirling, T. Soós and I. Pápai, *Angew. Chemie - Int. Ed.*, 2008, **47**, 2435–2438.
- (5) L. C. Brown, J. M. Hogg, M. Gilmore, L. Moura, S. Imberti, S. Gärtner, H. Q. N. Gunaratne, R. J. O'Donnell, N. Artioli, J. D. Holbrey and M. Swadźba-Kwaśny, *Chem. Commun.*, 2018, **54**, 8689–8692.

QUILL Quarterly Report

May 2019 – July 2019

Name:	Lucia McLaughlin		
Supervisor(s):	Dr Haresh Manyar		
Position:	QUILL Summer Student		
Start date:	1 st July 2019	Anticipated end date:	23 rd August 2019
Funding body:	QUILL		

Production of Alkyl Levulinates using Hybrid Organic-Inorganic materials based on Polyoxometalates and Ionic Liquids

Background

As a consequence of the depletion of fossil fuel resources and the further increasing requirement of fossil fuel derived energy in today's evolving society, it is essential to investigate and develop alternative methods of producing fuels, such as biofuels. Biofuels are environmentally benign and economically feasible as an alternative to fossil fuel derived fuels (such as petrol and diesel). There are many advantageous prospects of using biofuels, for example they can be considered carbon dioxide neutral (i.e. the biomass utilised such as plants respire to convert carbon dioxide to oxygen), provide a sustainable source of energy and can be produced from non-consumable biomass, therefore eliminating competition with the food-chain [1]. The optimisation of biofuels is essential in order to provide more efficient, cost effective and greener energy.

The addition of fuel additives is very beneficial when blended to biofuels. The fuel additive under investigation is Butyl Levulinate which has been found to have similar physical properties to petrol/diesel as well as having advantageous properties such as; high oxygen content, low water solubility, high-octane number, low toxicity, improved flow properties and reduces soot formation in engines [1]. The reaction to produce butyl levulinate is as follows (*figure 1 and 2*); Furfuryl alcohol reacts with n-butanol to form furfuryl butyl ether which then forms either the butyl levulinate or the 5,5-dibutoxy-2-pentanone which consequently forms the butyl levulinate (fuel additive).

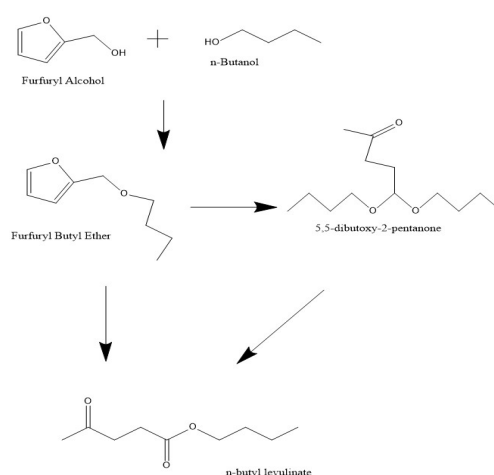


Figure 1 - Reaction pathway for the production of Butyl Levulinate using

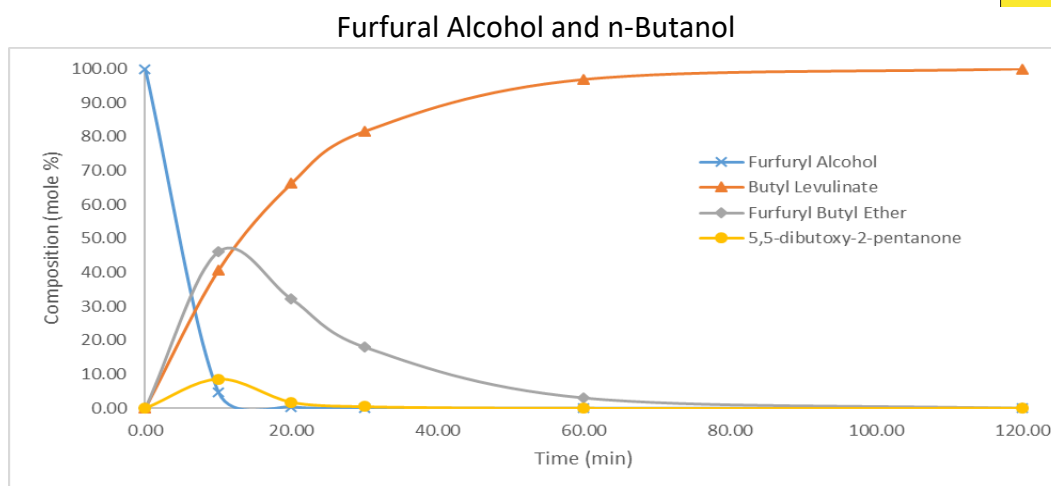


Figure 2 - Typical Reaction Profile

Figure 2 shows the typical reaction profile for the production of butyl levulinate and the reaction conditions are as follows; 1.15 mol of furfuryl alcohol, 0.05 mol n-butanol, 0.1g catalyst at 110°C in glass tube reactor with constant magnetic stirring at 1100 RPM.

Furfuryl alcohol is an advantageous feedstock in this process as it is inexpensive with an abundance of it in the chemical market, it does not compete with the food-chain, it is 100% atom economical and the products can be easily separated. It is produced from the hydrogenation of furfural which is produced from the hydrolysis and dehydration of the xylan found in lignocellulose.

The reaction requires the presence of an acid catalyst. Inexpensive and efficient mineral acids can be utilised for this reaction, however it has been found that they are extremely corrosive and therefore require neutralisation. Additionally, they are difficult to recycle and cause great damage to the environment. The 'greener' alternative to mineral acids is ionic liquids due to their low volatility and high thermal stability. Ionic liquids can be defined as compounds with melting points below 100°C consisting entirely of ions.

Operation of industrial scale production of alkyl levulinates from furfuryl alcohol currently takes place in China. However, the catalyst used by the factory is the corrosive mineral acid, hydrochloric acid which requires neutralisation thus producing salts. Furthermore, only a moderate yield is produced due to approximately 25% of the furfuryl alcohol being lost in uncontrolled polymerisation and during purification of the product. Further research indicates figures of furfuryl alcohol conversion ranging from 10-99% and selectivity to methyl levulinate from 1-98%. The homogeneous nature of these reactions also meant that the recovery of the ionic liquid was tedious.

Previous literature states that the DTP ($\text{H}_3\text{PW}_{12}\text{O}_{40}$) in the solid state is a strong Bronsted acid than the conventional HX, HY and H-ZSM5 zeolites. Polyoxometalate materials have interchangeable redox behaviours and also have the ability to act as electron reservoirs and donors whilst maintain their structure [2].

MCM-41 was used as an alternative catalyst support to K-10 as it holds many advantageous properties such as large surface area as a consequence of the regular arrangement of cylindrical mesopores that form a one dimensional pore system. As a result of this, the MCM-41 support catalyst performed significantly better than the respective K-10 catalyst.



Each of the components in the hybrid catalysts were separately analysed and developed in order to fully benefit from their useful properties and potential for catalysis.

K-10	Montmorillonite clay
NMP	N-methyl-2-pyrrolidone, C_5H_9NO
DTP	dodecatungstophosphoric acid, $H_3PW_{12}O_{40}$
MCM-41	Mobil Composition of Matter No.41, Mesoporous Silica

Objective of this work

The aim of this research is to identify a catalyst for the production of butyl levulinate using furfuryl alcohol as a feedstock which is fast, selective and recoverable. The catalysts were evaluated for the catalytic activity and selectivity to butyl levulinate.

A wide-range of hybrid organic-inorganic materials based on polyoxometalates and ionic liquids were prepared, tested and analysed. These catalysts included; $[NMP][HSO_4]$, K-10, $[NMP]_1 DTP$, $[NMP]_2 DTP$, $[NMP]_3 DTP$, DTP/K-10, DTP/MCM-41, $[NMP]_1 DTP/K-10$, $[NMP]_1 DTP/MCM-41$.

Progress to date

Catalyst Preparation

The preparation of catalysts DTP/K-10, DTP/MCM-41 were carried out via the wet impregnation method. This involved dissolving 0.4g DTP with methanol and slowly transferring dropwise onto each of the respective bases, ensuring that the contents were thoroughly mixed until dry before adding more of the DTP-methanol solution. The final solids were then dried at 120°C for 8 hours followed by calcination at 300°C for 3 hours.

The synthesis of the $[NMP]_1 DTP$, $[NMP]_2 DTP$, $[NMP]_3 DTP$ catalysts were carried out by preparing different molarity solutions of NMP in distilled water with set-amount solutions of DTP in distilled water. The aqueous solution of DTP was added dropwise to an aqueous solution of NMP for a duration of 10 minutes with constant stirring at 600 RPM. The mixture was then stirred at ambient temperature for the duration of 12 hours. The resulting mixture was then transported to a rotary evaporator for dehydration in vacuum to obtain final product.

The $[NMP]_1 DTP/MCM-41$ was prepared by making a 100 ml stock solution of 67.12 μ l NMP in 100 ml of methanol ensuring that the solution is well mixed. A 10 ml sample of this stock solution was then transferred into a round bottomed flask and suspended with 1 g of the 20 wt.% DTP/MCM-41 catalyst which had been previously made as stated above. The solution was mixed for 12 hours at 600 RPM and then placed in a rotary evaporator in order to remove the methanol present to obtain the final product.

Catalyst Reaction

Nine catalysts (as listed above) were all reacted under the same standard conditions as follows; 0.2 ml furfuryl alcohol was reacted with 0.05 ml n-dodecane and 4.2 ml butanol in order to achieve a 1:20 ratio. 0.2g of the respective catalysts were then added to this reaction mixture which was

heated at 110°C and continuously stirred at 1100 RPM over the duration of 5 hours in a glass tube reactor under batch conditions. The results were then analysed as follows using an Agilent Gas Chromatographer and the selectivity's of each respective catalyst at each hour was then determined.

Results

The selectivity of each respective catalyst was determined using the peak areas extracted from the gas chromatographer, the following formula was utilised.

$$\text{Selectivity} = \frac{\text{Peak area of Butyl Levulinate}}{\text{Total Peak Area of Spectrum}} \times 100$$

The graph and table 1 depicted below illustrates the relationship between selectivity of each of the respective catalysts over the duration of 5 hours under the standard conditions. It can be clearly seen that the [NMP]₁ DTP acquires the highest selectivity of 88.2% at 180 minutes. This is significantly larger than the other ionic, inorganic, organic and hybrid catalysts.

The ionic liquid catalyst [NMP]HSO₄ has a selectivity of approximately 50% to butyl levulinate over the duration of 5 hours. This is comparatively lower than the results depicted in literature. For example literature states selectivity of 98% using 0.3g of catalyst over a duration of 2 hours. This result should be repeated to ensure validity.

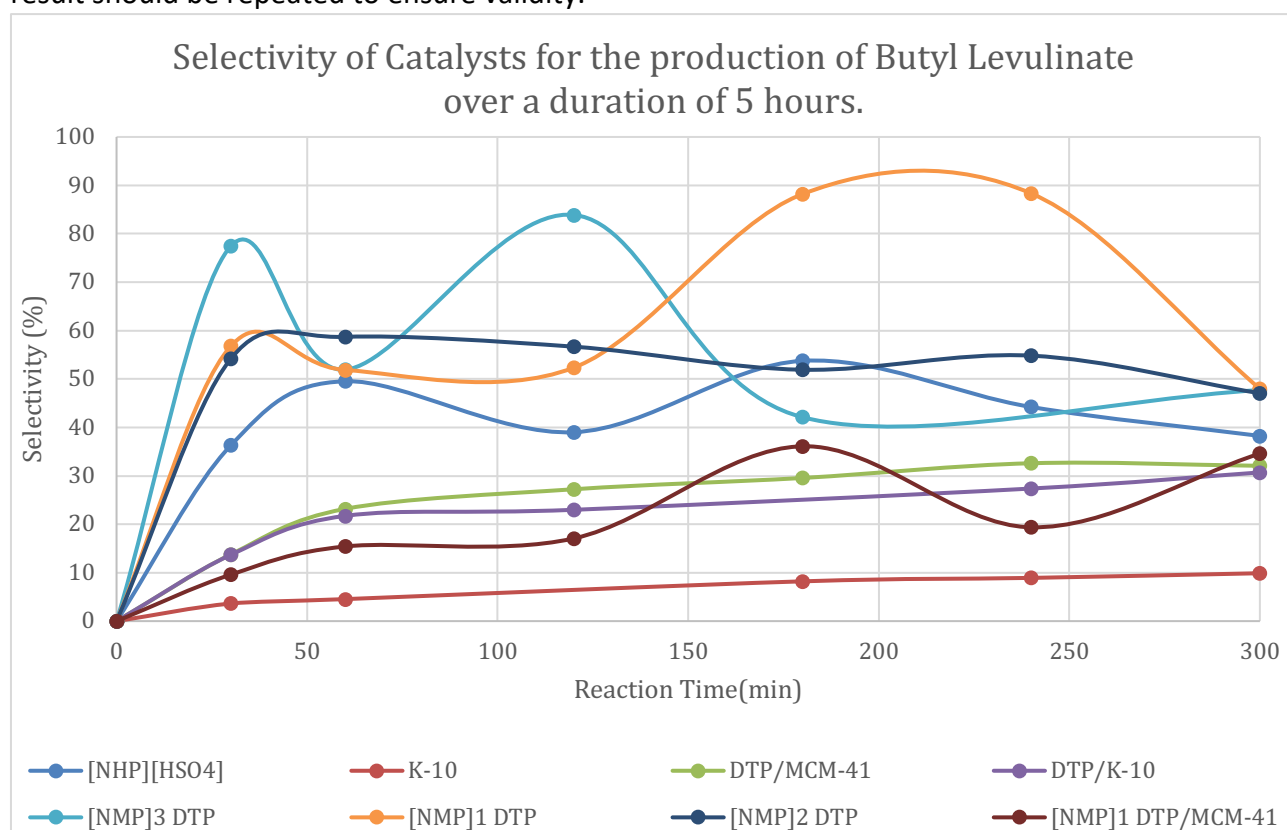


Figure 3 - Selectivity of all catalysts prepared and analysed against reaction time over a duration of 5 hours

Catalyst	Yield of Butyl Levulinate (%)
[NMP][HSO ₄]	38.3
K-10	9.9
DTP/MCM-41	32.1
DTP/K-10	30.7
[NMP] ₁ DTP	65.3
[NMP] ₂ DTP	47.1
[NMP] ₃ DTP	47.7
[NMP] ₁ DTP/MCM-41	34.6
[NMP]1/DTP 0.4g	58.5

Table 1 - Selectivity of each catalyst to butyl levulinate

Reaction conditions: 0.2 ml furfuryl alcohol, 4.2 ml n-butanol, 0.2g catalyst at 110°C in glass tube reactor with constant magnetic stirring at 1100rpm for 5 hours.

As seen from the graph above, the catalyst [NMP]₁DTP had a comparatively higher selectivity to butyl levulinate than [NMP]₂DTP and [NMP]₃DTP. Therefore, catalyst [NMP]₁DTP was further developed to catalyst [NMP]₁DTP/K-10 and [NMP]₁DTP/MCM-41 to further optimise the reaction.

Furthermore, it can be clearly seen that the DTP/MCM-41 acquires a higher selectivity to butyl levulinate than the DTP/K-10. This may be a consequence of the hexagonal array of the unidirectional and non-interconnecting pores that characterises the MCM-41 resulting in a comparatively much larger surface area than to the K-10 clay.

The [NMP]₁DTP/K-10 and [NMP]₁DTP/MCM-41 were prepared and developed obtaining smaller selectivity values in comparison to the [NMP]₁/DTP. Additionally, the [NMP]₁DTP produced a relatively high percentage yield in comparison to the other catalysts.

Recyclability

The catalyst was recovered by centrifugation whilst making sure that the catalyst does not lose its ability to catalyse the reaction. Therefore, the catalyst was recovered, washed and dried before being used in a subsequent reaction (under the same standard conditions). The performance of each reaction was then compared. Fresh catalyst was added to the reaction to ensure that the same amount of catalyst was used in each run. Alternatively, the catalyst mixture was washed with methanol and subsequently filtered and dried in an oven at 90°C for a duration of 12 hours.

The catalyst with the highest selectivity to butyl levulinate, [NMP]₁DTP was further analysed to determine its recyclability. 0.2g of the fresh catalyst was initially run and the amount recovered in the subsequent three reactions was 0.185g, 0.183g and 0.198g respectively. The increase in yield in the third run may have been a consequence of impurities being present within the catalyst, therefore this must be repeated to ensure validity within the results.

The results of the recyclability of [NMP]₁DTP are as follows;

	Yield of Butyl Levulinate (%)	Percentage Recovered at End of Reaction (%)
Fresh Sample	43.4	92.5
Run 1	74.5	93.5
Run 2	33.0	99.0

Table 2 - Recyclability analysis of $[NMP]_1$ DTP

Characterisations of Catalysts

The new inorganic-organic hybrid catalysts are prepared and characterised by FT-IR and XRD. Each of the different inorganic parts of the hybrids catalysts were investigated to show their different molecular structures.

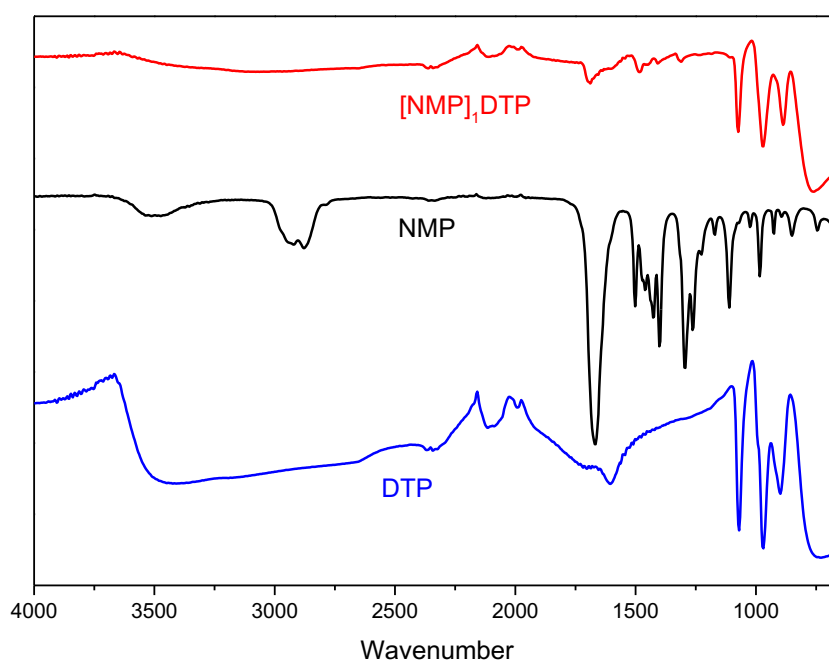


Figure 4 - FT-IR Data for N-methyl-2-pyrrolidone, unsupported DTP and the $[NMP]_1$ DTP Sa

The FT-IR spectrum of neat DTP shows characteristic bands for the Keggin structure from 700 to 1100 cm^{-1} . The peaks present in the spectrum at 1069 cm^{-1} , 970 cm^{-1} , 899 cm^{-1} and 760 cm^{-1} are assignable respectively to the vibration of $\nu(\text{P-O})$, terminal $\nu(\text{W=O})$, corner $\nu(\text{W-O-W})$ and edge-sharing $\nu(\text{W-O-W})$ [3].

For the salt $[NMP]_1$ DTP the Keggin structure of DTP remains intact but with a blue shift of 1069 cm^{-1} to 1073 cm^{-1} , and a red shift from 899 cm^{-1} to 887 cm^{-1} .

The FT-IR of neat NMP shows a peak at 1670 cm^{-1} associated with carbonyl stretching, with a shift in this peak to 1687 cm^{-1} observed for $[NMP]_1$ DTP. From the FT-IR data we can determine that the

original structures of both components are retained, with shift in IR values indicating that ionic bonds are being formed between NMP cation and the DTP anion [4].

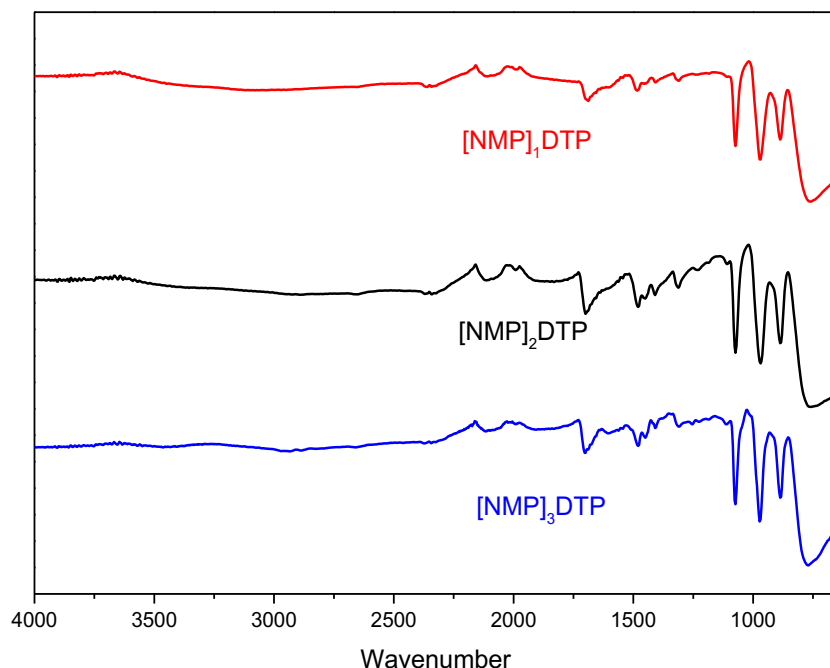


Figure 5 - FT-IR Data for N-methyl-2-pyrrolidone DTP salts

For all the salts of [NMP]DTP we can see that the characteristic peaks associated with the Keggin structure of DTP and the carbonyl stretching peak of NMP are present. This infers that the structure of both components remains intact regardless of the degree of substitution.

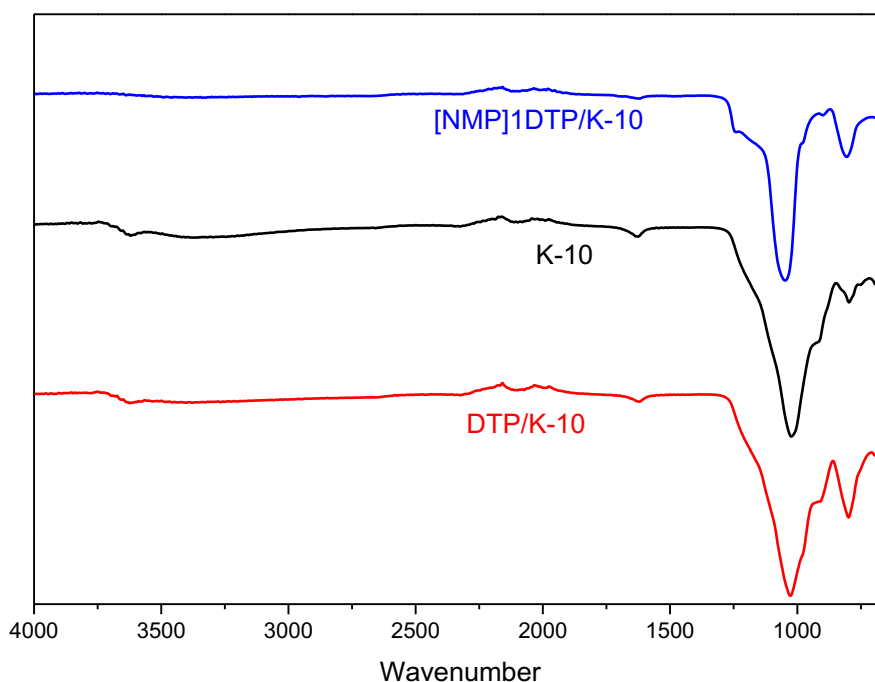


Figure 6 - K-10 clay supported Catalysts

From the FT-IR of pure K-10 montmorillonite clay we can see an intense band at 1019 cm^{-1} associated with Si-O out-of-plane stretching. The next most intense peak at 795 cm^{-1} corresponds

to the platy form of disordered tridymite (form of quartz). Bands at 3626 cm^{-1} and 1639 cm^{-1} correspond to the stretching and bending of O-H from water present in the clay. The band at 915 cm^{-1} is associated with AlAlOH bending vibration [5]. It can be noted from the spectra that DTP/K-10 and also [NMP]₁DTP/K-10 that the spectrum is highly similar to that of the support material.

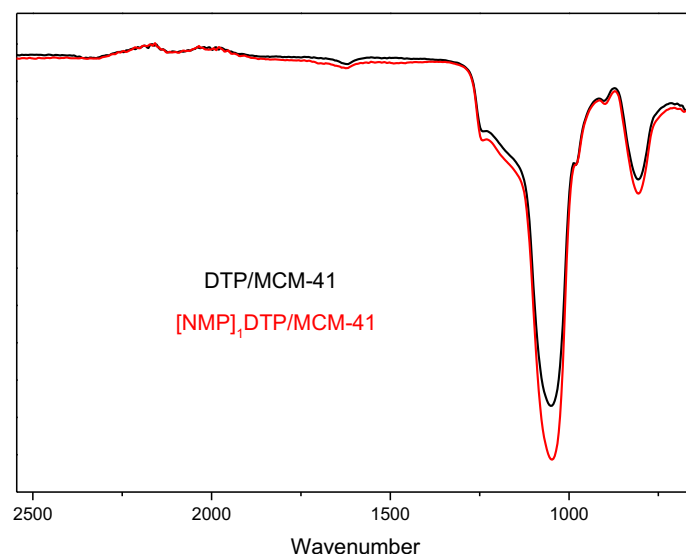


Figure 7 - MCM-41 supported DTP and [NMP]₁DTP/MCM-41

Similar to the K-10 supported catalysts, the overall spectra for the supported catalysts is highly similar to that of neat MCM-41.

Conclusions and future work

From results obtained above it can be clearly seen that the [NMP]₁DTP hybrid catalyst has the highest selectivity in comparison to the other ionic, inorganic-organic and hybrid catalysts. [NMP]₁DTP was recovered and reused for three runs. From this report a new catalyst was developed with simple preparation of the catalyst, mild reaction conditions and superior selectivity's.

Future Work

Optimisation of the reactions is key to produce a cleaner, sustainable and more cost effective biofuel. The reaction can be optimised with regards to; catalyst loading, mole ratio of furfuryl alcohol to n-butanol, speed of agitation, temperature and the effect of water on the efficiency of the catalyst. Additionally, using different alcohols such as methanol instead of butanol. Scale-up of the lab findings must be closely examined and the reaction scale must be increased in steps with additional focus on safety (e.g. Chemical storage, transportation, reactors, thermal runaways etc.).

References

- (1) Single pot conversion of furfuryl alcohol to levulinic esters and γ -valerolactone in the presence of sulfonic acid functionalized IIs and metal catalysts *Rhode et al*, *Green Chem*, 2013, 15, 2540
- (2) Svetlana Ivanova (2014) 'Hybrid Organic-Inorganic Materials Based on Polyoxometalates and Ionic Liquids and Their Application in Catalysis', *ISRN Chemical Engineering*, 1(Article ID 963792,), pp. 13.]
- (3) Tiwari MS, Yadav GD. Novel aluminium exchanged dodecatungstophosphoric acid supported on K-10 clay as catalyst: Benzoylation of diphenyloxide with benzoic anhydride. *RSC Adv*.



2016;6(54):49091-49100. <http://dx.doi.org/10.1039/C6RA05379C>.
10.1039/C6RA05379C.

doi:

- (4) Zhang W, Leng Y, Zhao P, Wang J, Zhu D, Huang J. Heteropolyacid salts of N-methyl-2-pyrrolidonium as highly efficient and reusable catalysts for prins reactions of styrenes with formalin. *Green Chem.* 2011;13(4):832-834. <http://dx.doi.org/10.1039/C0GC00729C>. doi: 10.1039/C0GC00729C.
- (5) Wang F, Liu J, Li H, Liu C, Yang R, Dong W. Conversion of cellulose to lactic acid catalyzed by erbium-exchanged montmorillonite K10. *Green Chem.* 2015;17(4):2455-2463. <http://dx.doi.org/10.1039/C4GC02131B>. doi: 10.1039/C4GC02131B.

QUILL Quarterly Report

May - July 2019

Name:	Peter McNeice		
Supervisor(s):	Dr Andrew Marr, Dr Patricia Marr		
Position:	PhD student		
Start date:	October 2016	Anticipated end date:	July 2020
Funding body:	QUILL IAB		

Base Stable and Basic Ionic Liquids

Background

The imidazolium cation is the most common cation in ionic liquids due to its acid stability, thermal stability and oxidative stability.¹ Unfortunately, it can be extremely sensitive to base. The most acidic position is the C2 proton which deprotonates to form a carbene (Figure 9). The instability of the C2 position in base was demonstrated in 1964 with heavy water buffers causing deuteration at the C2 position.² The acidity of this proton limits the use in base catalysed reactions. This has been investigated by Aggarwal *et al.*³ who found that [BMIM][Cl] was deprotonated to form a carbene which went on to attack the aldehyde component of a Baylis-Hillman reaction, reducing the yield. They found that bases with pK_a as low as 8 or 9 could generate a carbene.

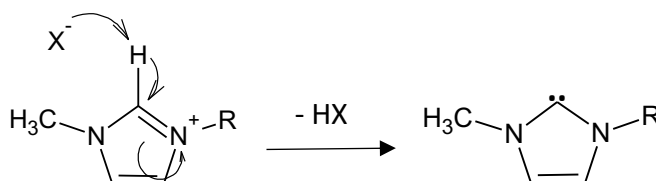


Figure 9: Deprotonation of an imidazolium cation to form a carbene. X^- can be the anion or a base.

When an ionic liquid is able to catalyse a reaction, it is called a functionalised ionic liquid (FIL), previously known as a task specific ionic liquid (TSIL).⁴ These materials can be created due to the tuneable properties of ionic liquids and have the potential to cut down on auxiliary stoichiometric catalysts and prevent the formation of salts.

Ionic liquids can be basic due to the presence of a Brønsted basic (proton accepting) anion. Examples include ionic liquids with OH^- ,⁵ imidazolate ($[Im]^-$),⁶ carboxylate,^{7,8} amino acids⁹ and dicyanamide ($[DCA]^-$)¹⁰ as anions (Figure 10).

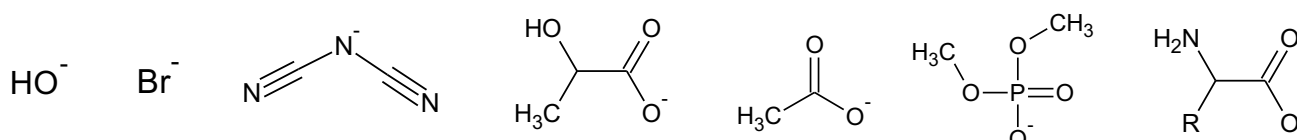


Figure 10: Some Brønsted basic anions for ionic liquids.

Ionic liquids with basic anions often suffer from instability. The anion is able to attack the cation to form two neutral species as shown in Figure 9. Strong bases such as halide ions and OH^- in particular suffer from this effect.

Heterogenising ionic liquids can increase their stability and allows for simple separation of the ionic liquid catalyst from the reaction mixture. Hydrotalcites (layered double hydroxides) are clay-like materials with the general formula $[M^{II}_{1-x}M^{III}_x(OH)_2]^{x+}(A^{n-})_{x/n} \cdot mH_2O$ where M^{II} and M^{III} are di and tri-valent metal ions which form the outer layers. A^- is an inter-layer ion such as Cl^- , $(CO_3)^{2-}$, $(NO_3)^-$ or $(SO_4)^{2-}$

Figure 11).¹¹ Hydrotalcites have found use in catalysis,¹² polymer science¹³ and electrochemistry,¹⁴ amongst other applications.¹⁵ The interlayer anions can be ion exchanged, which allows them to be intercalated by ionic liquid anions to form ionic liquid hydrotalcite composites.¹⁶

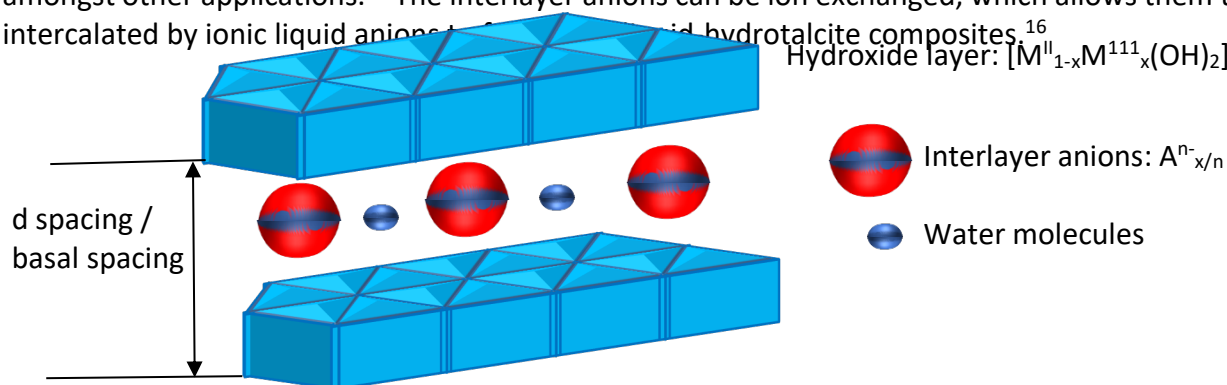


Figure 11: A representation of the structure of hydrotalcite

Objective of this work

The overall aim of this project is to synthesise functionalised ionic liquids which are base stable and basic. Basic ionic liquids will be able to act as both solvent and catalyst for reactions, which will eliminate waste. Stability is key for catalysis as well as recovery of the ionic liquid.

Progress to date

In a previous report¹⁷ ionic liquid hydrotalcite (IL-HT) catalysts were synthesised using $[P_{66614}][C_8SO_3]_x[O^iPr]_{1-x}$ to increase the basal spacing, hydrophobicity and basicity of hydrotalcite. An initial test of the catalytic activity of the IL-HT catalysts was the Aldol condensation between benzaldehyde and acetophenone under neat conditions. The initial yields were promising (45-75 % after 1 hour) but the yields decreased significantly on the second and third use. This report details further work on these IL-HT catalysts to allow for their successful recovery and reuse.

Table 1: Crude yield of HT and IL-HT catalysed Aldol condensation between benzaldehyde and acetophenone using solvent.

Entry	Catalyst	Crude Yield / % ^a (\pm , SD)		
		1 st Run	2 nd Run	3 rd Run
1	Hydrotalcite (HT)	30 (0)	9 (0)	0 (0)
2	$[P_{66614}][C_8SO_3]$ -HT (IL-HT1)	33 (1)	15 (2)	2 (2)
3	$[P_{66614}][C_8SO_3]_{0.9}[O^iPr]_{0.1}$ -HT (IL-HT2)	35 (6)	15 (5)	0 (0)
4	$[P_{66614}][C_8SO_3]_{0.74}[O^iPr]_{0.26}$ -HT (IL-HT3)	41 (0)	8 (1)	0 (0)
5	$[P_{66614}][C_8SO_3]_{0.48}[O^iPr]_{0.52}$ -HT (IL-HT4)	22 (4)	9 (5)	0 (0)



Conditions: Benzaldehyde (0.104 g, 0.97 mmol, 1 eq.), acetophenone (0.287 g, 2.39 mmol, 2.5 eq.), IL-HT (0.021, 20 wt. % of benzaldehyde), sulfolane (0.300 g, 1:1 (w/w) with reagents) (140 °C, stir rate 500 RPM and time 1 h). ^a Obtained from ¹H NMR against a known mass of ethyl trifluoroacetate, value is an average of three reactions.

Table 1 shows the results when sulfolane was used as a solvent to improve the mixing of the catalyst with the reagents and to act as a diluent for heat, possibly protecting the catalyst from deactivation. The crude yield of the reactions decreased compared to the neat reaction,¹⁷ probably due to the reagents being diluted. **IL-HT3** is the best performing catalyst (Table 1 entry 4) and only slight differences in crude yield are seen between the other catalysts (Table 1 entries 1-3, 5). The yield still decreases significantly after the first reaction. The decrease is proportionately less than in the neat reaction¹⁷ but solvent has not had a significant effect in aiding catalyst recycling.

The reaction was then performed under a flow of nitrogen (Table 2). It was thought that at the high reaction temperature, air may be contributing to the deactivation of the catalyst. This was reported by Climent *et. al.*¹⁸ who found benzaldehyde was oxidised to benzoic acid under air which then neutralised the basic sites of hydrotalcite. The crude yield for the first reactions (Table 2) were similar to those obtained without N₂ (Table 1) except for **IL-HT4** (Table 2 entry 5). The crude yield of **IL-HT4** has doubled using N₂. As it has the highest proportion of [OⁱPr]⁻, without the flow of N₂ the catalyst may be more susceptible to deactivation, either through decomposition of the ionic liquid or attack on the hydrotalcite structure by [OⁱPr]⁻. The flow of N₂ may prevent this, allowing the larger proportion of [OⁱPr]⁻ to have a positive effect on the reaction rather than a negative effect on the catalyst's stability. If benzaldehyde oxidation is a factor then it may be occurring more when **IL-HT4** is the catalyst compared to the other IL-HTs. There is a large improvement in catalyst recycling under a flow of N₂. A slight increase in crude yield is observed after the second reaction for **IL-HT1**, **IL-HT2**, and **IL-HT3** (Table 2 entries 2, 3, 4) but it is within or near the calculated standard deviation. **IL-HT1**, **IL-HT2**, and **IL-HT3** (Table 2 entries 2, 3, 4) have retained their activity after three reactions better than unmodified **HT**. This would indicate the ionic liquid modification is important for stabilising the hydrotalcite structure and is not just important for improving the crude yield. **IL-HT4** (Table 2 entry 5) experiences a relatively large decrease in crude yield after the 3rd reaction. This is possibly due to the high proportion of [OⁱPr]⁻ in the composite causing decomposition or deactivation, despite the extra protection provided by the flow of N₂ discussed above. **IL-HT2**, and **IL-HT3** (Table 2 entries 3, 4) have best retained their catalytic ability after three reactions and do not display any final difference in activity compared to the first reaction. Despite having lower initial crude yields than **IL-HT4** these are overall the best performing catalysts.

Table 2: Crude yield of HT and IL-HT catalysed Aldol condensation between benzaldehyde and acetophenone using solvent and a flow of nitrogen.

Entry	Catalyst	Crude Yield / % ^a (±, SD)		
		1 st Run	2 nd Run	3 rd Run
1	Hydrotalcite (HT)	36 (3)	36 (3)	19 (2)
2	[P ₆₆₆₁₄][C ₈ SO ₃]-HT (IL-HT1)	30 (1)	44 (3)	29 (2)
3	[P ₆₆₆₁₄][C ₈ SO ₃] _{0.9} [O ⁱ Pr] _{0.1} -HT (IL-HT2)	30 (2)	33 (6)	20 (6)
4	[P ₆₆₆₁₄][C ₈ SO ₃] _{0.74} [O ⁱ Pr] _{0.26} -HT (IL-HT3)	30 (3)	37 (2)	30 (1)
5	[P ₆₆₆₁₄][C ₈ SO ₃] _{0.48} [O ⁱ Pr] _{0.52} -HT (IL-HT4)	45 (7)	38 (8)	19 (7)

Conditions: Benzaldehyde (0.102 g, 0.96 mmol, 1 eq.), acetophenone (0.288 g, 2.40 mmol, 2.5 eq.), IL-HT (0.021, 20 wt. % of benzaldehyde), sulfolane (0.391 g, 1:1 (w/w) with reagents) (N₂, 140 °C,



stir rate 500 RPM and time 1 h). ^a Obtained from ¹H NMR against a known mass of ethyl trifluoroacetate, value is an average of three reactions.

In an attempt to obtain quantitative yields the reaction time was increased to 6 hours (Table 3). After the first reaction **IL-HT3** achieved the highest crude yield (Table 3 entry 5) whilst **IL-HT4** and **HT** achieved only slightly lower yields (Table 3 entries 6, 2). **IL-HT1** and **IL-HT2** had lower yields (Table 3 entries 3, 4). It is possible that these ionic liquids block the basic sites of hydrotalcite without providing enough [OⁱPr]⁻ to effectively catalyse the reaction. **IL-HT3** (Table 3 entry 5) best maintains its catalytic ability after three reactions but still has a large decrease in activity. The longer reaction time appears to cause deactivation of the catalysts. It would be better to use the catalysts in shorter reactions, sacrificing the higher yields, if it meant that the catalysts were able to be reused successfully.

Table 3: Crude yield of HT and IL-HT catalysed 6 hour Aldol condensation between benzaldehyde and acetophenone using solvent and a flow of nitrogen.

Entry	Catalyst	Crude Yield / % ^a (±, SD)		
		1 st Run	2 nd Run	3 rd Run
1	None	5 (0)	NA	NA
2	Hydrotalcite (HT)	90 (7)	70 (5)	13 (4)
3	[P ₆₆₆₁₄][C ₈ SO ₃]-HT (IL-HT1)	77 (2)	39 (2)	8 (3)
4	[P ₆₆₆₁₄][C ₈ SO ₃] _{0.9} [O ⁱ Pr] _{0.1} -HT (IL-HT2)	75 (5)	66 (0)	9 (5)
5	[P ₆₆₆₁₄][C ₈ SO ₃] _{0.74} [O ⁱ Pr] _{0.26} -HT (IL-HT3)	96 (0)	83 (0)	42 (2)
6	[P ₆₆₆₁₄][C ₈ SO ₃] _{0.48} [O ⁱ Pr] _{0.52} -HT (IL-HT4)	90 (7)	71 (5)	7 (2)

Conditions: Benzaldehyde (0.104 g, 0.98 mmol, 1 eq.), acetophenone (0.308 g, 2.57 mmol, 2.5 eq.), IL-HT (0.021, 20 wt. % of benzaldehyde), sulfolane (0.407 g, 1:1 (w/w) with reagents) (N₂, 140 °C, stir rate 500 RPM and time 6 h). ^a Obtained from ¹H NMR against a known mass of ethyl trifluoroacetate, value is an average of three reactions.

Conclusions and Future work

IL-HT catalysed reactions have been performed under various conditions to assess whether IL-HTs can be recovered and reused after a reaction. Using solvent slightly improves the yield in subsequent reactions but a low yield is still achieved after the 3rd use. A flow of N₂ allows **IL-HT2** and **IL-HT3** to be used for a total of three 1 hour reactions without a decrease in crude yield. When the reaction time is increased to 6 hours the IL-HTs can produce almost quantitative crude yields but experience a large decrease in yield in subsequent reactions. A shorter reaction time may be ideal for these catalysts. A lower yield is achieved but this allows the catalyst to be recycled.

Further work should be performed on the IL-HT catalysts to achieve quantitative yields after several uses of the catalysts. This may involve performing reactions at lower temperatures for a longer time to prevent catalyst deactivation. Once optimum conditions are found for high yields and good recyclability the IL-HTs can be modified with metal nanoparticles. Hydrotalcite has already been shown to support metal nanoparticles for hydrogenation,¹⁹ transamination²⁰ and C-C bond coupling reactions²¹ amongst others. The activity may be improved using IL-HTs and it would potentially allow the base and metal catalyst to be recovered in one material, reducing waste and saving money.

References

- (1) S. T. Handy, *Curr. Org. Chem.*, 2005, **9**, 959-988.
- (2) R. A. Olofson, W. R. Thompson, J. S. Michelman, *J. Am. Chem. Soc.*, 1964, **86**, 1865-1866.
- (3) V. K. Aggarwal, I. Emme, A. Mereu, *Chem. Commun.*, 2002, 1612-1613.
- (4) A. C. Cole, J. L. Jensen, I. Ntai, K. Loan, T. Tran, J. K. Weaver, D. C. Forbes, J. H. J. Davis, *J. Am. Chem. Soc.*, 2002, **124**, 5962-5963.
- (5) J.-M. Xu, Q. Wu, Q.-Y. Zhang, F. Zhang, X.-F. Lin, *Eur. J. Org. Chem.*, 2007, 1798-1802.
- (6) H. Luo, Z. Zhai, W. Fan, W. Cui, G. Nan, Z. Li, *Ind. Eng. Chem. Res.*, 2015, **54**, 4923-4928.
- (7) Y. Liu, Y. Huang, P.-O. Boamah, L. Cao, Q. Zhang, Z. Lu, H. Li, *J. Appl. Polym. Sci.*, 2015, **132**, 41727.
- (8) A. Cieniecka-Rostiewicz, K. Kita, A. Fojutowski, J. Nawrot, K. Materna, J. Pernak, *Chem. Eur. J.*, 2008, **14**, 9305-9311.
- (9) H. Peng, Y. Zhou, J. Liu, H. Zhang, C. Xia, X. Zhou, *RSC Adv.*, 2013, **3**, 6859-6864.
- (10) D. R. MacFarlane, S. A. Forsyth, J. Golding, G. B. Deacon, *Green Chem.*, 2002, **4**, 444-448.
- (11) W. T. Reichle, *Solid State Ionics*, 1986, **22**, 135-141.
- (12) S. Nagasaki, M. Halma, A. Bail, G. G. C. Arizaga, F. Wypych, *Colloid Interface. Sci.*, 2005, **281**, 417-423.
- (13) S. O'Leary, D. O'Hare, G. Seeley, *Chem. Commun.*, 2002, **0**, 1506-1507.
- (14) Y. Wang, W. Yang, J. Yang, *Electrochem. Solid-State Lett.*, 2007, **10**, A233-A236.
- (15) Q. Wang, D. O'Hare, *Chem Rev.*, 2012, **112**, 4124-4155.
- (16) S. Livi, V. Bugatti, L. Estevez, J. Duchet-Rumeau, E. P. Giannelis, *J. Colloid Interface Sci.*, 2012, **388**, 123-129.
- (17) P. McNeice, *Base Stable and Basic Ionic Liquids*, QUILL Quarterly Report November 2018 - January 2019, Unpublished, February 2019.
- (18) M. J. Climent, A. Corma, S. Iborra, J. Primo, *J. Catal.*, 1995, **151**, 60-66.
- (19) Á Mastalir, Z. Kirá, *J. Catal.*, 2003, **2**, 372-381.
- (20) D. Ainembabazi, N. An, J. C. Manayil, K. Wilson, A. F. Lee, A. M. Voutchkova-Kostal, *ACS Catal.*, 2019, **9**, 1055-1065.
- (21) M. L. Kantam, S. Roy, M. Roy, B. Sreedhar, B. M. Choudary, R. L. De, *J. Mol. Catal. A: Chem.*, 2007, **273**, 26-31.

QUILL Quarterly Report

May 2019 – July 2019

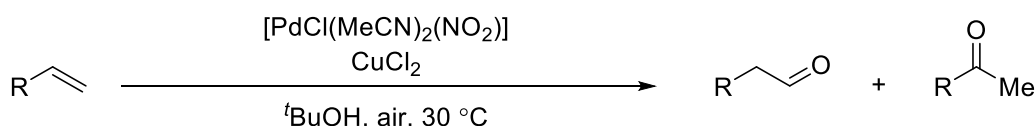
Name:	Rebecca Millar		
Supervisor(s):	Dr Mark Muldoon		
Position:	Undergraduate Summer Student		
Start date:	27/05/2019	Anticipated end date:	20/09/2019
Funding body:	Royal Society of Chemistry & QUILL		

Investigation of Pd(II) Catalysed Oxidation Reactions

Background

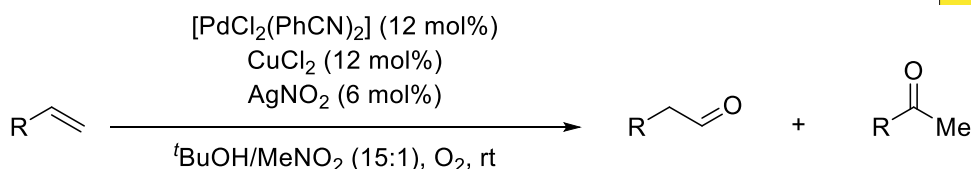
Oxidation of terminal alkenes to carbonyls is a fundamental and highly useful reaction. The industrial Wacker process of ethene to acetaldehyde utilises palladium (II) salts as the catalysts. The oxidation of longer chain alkenes (commonly called the Wacker-Tsuji oxidation reaction) predominantly produces the methyl-ketone product. Anti-Markovnikov (AM) selective Wacker oxidation to produce the aldehyde product is very also very desirable, given the utility of aldehydes, but these catalytic systems are not well developed or efficient. As early as the mid-1980s, aldehyde selectivity was achieved under Wacker-Tsuji conditions, however high selectivity was only achieved for a limited range of substrates, mostly those containing bulky groups close to the alkene.

Attempts to obtain aldehyde selectivity in Wacker oxidations of unbiased alkenes included research conducted by Feringa and co-workers. In 1986, they discovered aldehydes were the major products of the catalytic oxidation of alk-1-enes with air using a catalyst that comprises $(\text{MeCN})_2\text{Pd}(\text{NO}_2)\text{Cl}$ and CuCl_2 conducted in *tert*-butanol as the solvent (**Scheme 1**). This provided encouraging results for aldehyde selectivity (2.3:1) in spite of poor yield (>20%).



Scheme 1 - Feringa's reaction conditions for one of the first anti-Markovnikov oxidation reactions.

In recent years, there have been advances in this area and catalyst-controlled systems have been developed, which have good aldehyde selectivity for a wide range of substrates. Grubbs and co-workers developed the system illustrated in **Scheme 2**. In most cases, these catalyst systems involve NO_x as a key oxidant, therefore, nitrites are employed. Grubbs suggested that *tert*-butyl nitrite was the highly aldehyde-selective species component which may be generated in situ. In one experiment, Grubbs combined *tert*-butyl nitrite with PdCl_2 and CuCl_2 and observed significantly increased selectivity (**Figure 1, Entry 3**). They reasoned that other nitrite sources may enable a more efficient pathway to the selective catalytic species and as a result they discovered AgNO_2 provided the significant improvement they were looking for (**Figure 1, Entries 7 & 8**). Additionally, MeNO_2 as a co-solvent was found to give enhance the performance even further.



Scheme 2 - Reaction conditions developed by Grubb and co-workers

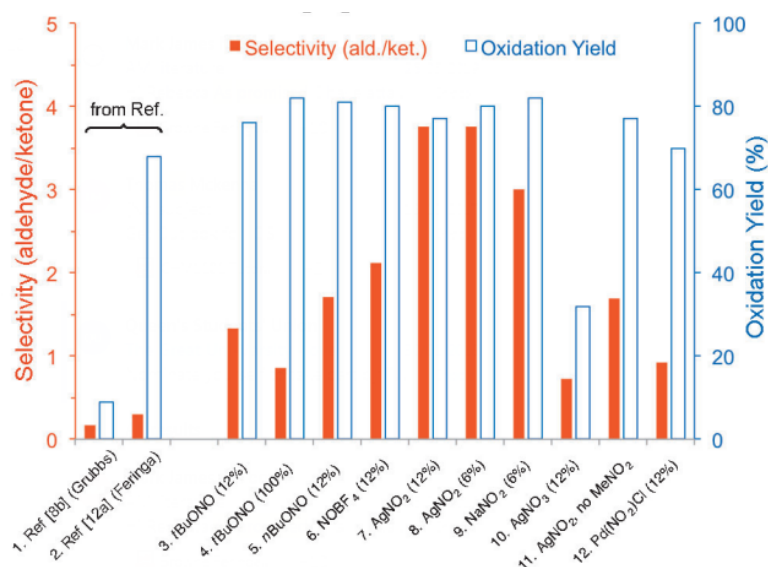
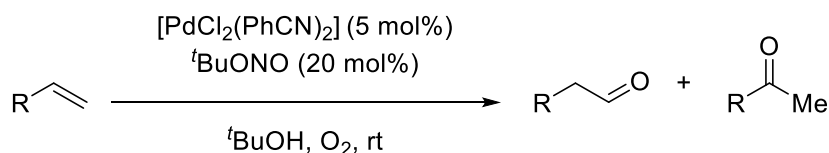


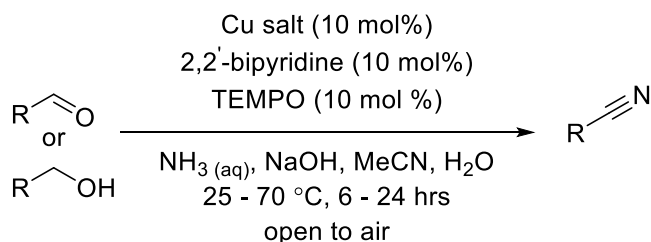
Figure 12 - Catalyst optimisation by Grubbs and Co-workers found that AgNO₂ was the most aldehyde selective nitrite salt. Reproduced from the Reference **Error! Bookmark not defined.**

Kang and co-workers modified Grubbs' methodology to remove silver and copper salts and developed a system which used tert-butyl nitrite, a convenient organic NO_x-source, which would replace inorganic NO₂-salts as shown below in **Scheme 3**. This allowed for mechanistic studies based on the Pd (II) salt without the influence of either copper or silver. This system could achieve aldehyde regioselectivity of up to 30:1.



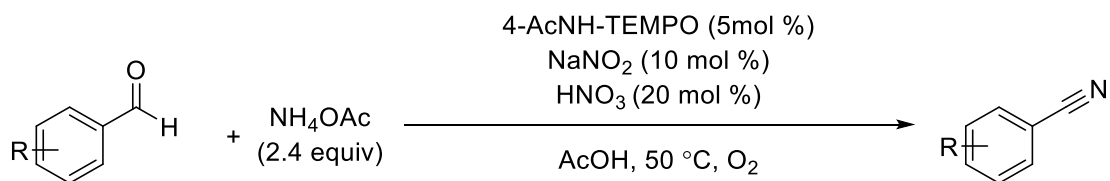
Scheme 3 - Kang's modification of the previous Feringa and Grubbs methodologies

Aldehydes are valuable building blocks and can be used for further transformations. For example, Muldoon and co-workers previously formed nitriles from aldehydes and alcohols using a Cu/TEMPO catalyst and aqueous ammonia (**Scheme 4**). In this reaction, the aldehyde or alcohol reacts with ammonia to form the imine and this is then oxidised to the nitrile by the catalyst. The system was tolerant of many functional groups, with isolated yields of up to 96% being achieved,



Scheme 4 - The Muldoon group's Copper/TEMPO catalysed synthesis of nitriles from aldehydes or alcohols using aqueous ammonia and with air as the oxidant.

Since their work there have been more recent advancements. In 2015, Kim and co-workers developed a nitroxyl/NO_x catalyst system. In the presence of a catalytic amount of 4-AcNH-TEMPO (4-acetamido-2,2,6,6-tetramethylpiperidine-N-oxyl), NaNO₂, and HNO₃, aromatic benzaldehydes bearing a variety of functional groups underwent condensation with NH₄OAc and following aerobic oxidation to produce nitriles selectively under an O₂ balloon. They were able to achieve up to 99% yield of the nitrile product. This system did not utilise copper complexes, however the substrate scope was limited to aromatic aldehydes. The use of NO_x is an indication that TEMPO is oxidised to the corresponding oxoammonium salt and this is the active 2-electron oxidant for the reaction.



Scheme 5 - Aerobic oxidative conversion of aromatic aldehydes to nitriles using a nitroxyl/NO_x catalyst system.

Objective of this work

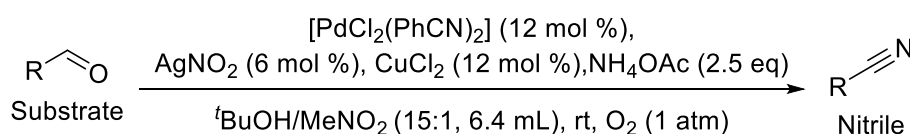
This summer project has looked at two different aspects. Firstly, can alkenes be converted to nitriles *via* a cascade reaction where Pd Anti-Markovnikov type catalysts salt will carry the reaction right through to the nitrile, when ammonia is present. Secondly, the Anti-Markovnikov catalyst systems to-date have all been relatively similar and there is scope for improvement. Different conditions (e.g. solvent effects) were examined to explore if catalyst efficiency could be improved.

Progress to date

The starting point of these investigations was to replicate some of the research that had previously been conducted by the Grubbs and Kang Groups.**Error! Bookmark not defined.** This would enable us to validate our experimental methods and compare results for future amendments to these respective catalytic systems. With regards to making nitriles, such cascade reactions could be carried out a few different ways. Ammonia and any required co-catalysts could be added at the start of the alkene oxidation. The theory was that once the aldehyde was synthesised, it could immediately be converted to the imine and then the nitrile. Unfortunately, nitrile synthesis, from simply adding ammonium acetate to the reaction mixture at the start of the reaction with styrene, was unsuccessful. Alternatively, ammonia and any additional catalysts could be added to the flask once the AM Wacker oxidation reaction was complete.

In order to find the best route for nitrile synthesis, we decided to start with the corresponding aldehyde as the starting material. This would simplify the studies and clearly demonstrate if the catalysts could convert aldehydes to nitriles. The Grubbs system was tested initially (**Table 1**). The idea was to determine whether the Pd (II) catalyst could take the aldehyde to the nitrile. It is evident that the aromaticity benefits this reaction.

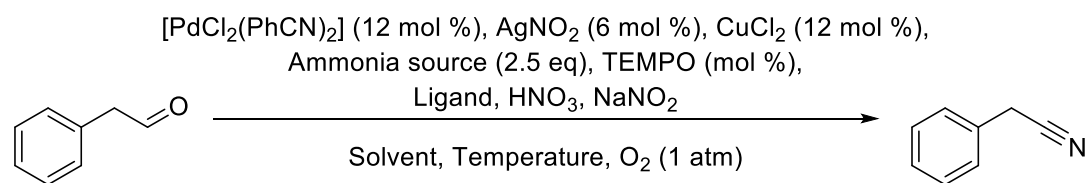
Table 4 - Nitrile synthesis beginning with the respective aldehyde using the Grubbs conditions as a basis and adding ammonium acetate to the reaction mixture.



Entry	Substrate	Yield (%)	Time (hr)
1	Phenylacetaldehyde	0	5
2	Benzaldehyde	20	3
3	Octanal	0	2.5

Upon little success with non-aromatic aldehydes, the investigation turned to testing different ammonium salts and examining the effects of altering the temperature range. The stable radical, TEMPO, was also tested as an additive alongside different ligands. Additionally, the solvent effects were tested with varying degrees of success (**Table 2**). It was found that nitrile product could only be achieved in the presence of a TEMPO co-catalyst.

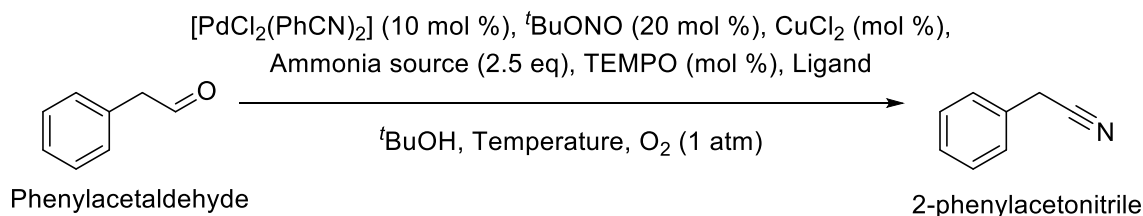
Table 5 - Exploring the conversion of phenylacetaldehyde to 2-phenylacetonitrile



Entry	Solvent	TEMPO (mol %)	Ligand	HNO ₃ (mol%)	NaNO ₃ (mol%)	Temp (deg C)	Ammonia source	Yield (%)	Time (hr)
1	tBuOH/MeNO ₂ (15:1)	0	0	0	0	rt	NH ₄ Br	x	2
2	tBuOH/MeNO ₂ (15:1)	0	0	0	0	rt	NH ₄ Cl	x	2
3	tBuOH/MeNO ₂ (15:1)	5	0	0	0	70	NH ₄ OAc	x	6
4	tBuOH/MeNO ₂ (15:1)	5	0	0	0	50	NH ₄ OAc	6	12
5	tBuOH/MeNO ₂ (15:1)	10	0	0	0	50	NH ₄ OAc	3	19.75
6	tBuOH/MeNO ₂ (15:1)	20	0	0	0	50	NH ₄ OAc	2	18.75
7	tBuOH/MeNO ₂ (15:1)	10	0	0	0	70	NH ₄ OAc	3	6
8	tBuOH/MeNO ₂ (15:1)	10	Bipy (10 mol%)	0	0	rt	NH ₄ OAc	9	23.5
9	tBuOH/MeNO ₂ (15:1)	10	Bipy (10 mol%)	0	0	50	NH ₄ OAc	5	23.5
10	tBuOH/MeNO ₂ (15:1)	10	Bipy (10 mol%)	0	0	50-70	NH ₄ OAc	9	23.5
11	tBuOH/MeNO ₂ (15:1)	0	0	20	10	50	NH ₄ OAc	x	17.5
12	MeCN	10	Bipy (10 mol%)	0	0	rt	NH ₄ OAc	8	24
13	EtOH	10	Bipy (10 mol%)	0	0	rt	NH ₄ OAc	9	24
14	HFIP	10	Bipy (10 mol%)	0	0	rt	NH ₄ OAc	1	24

Investigations, then, began using the Kang system with the addition of TEMPO while varying the temperature and the addition of ligands. Increased the reactivity yielded a current maximum of 13% nitrile (**Table 3**). It can be concluded that elevated temperatures had little influence on the reaction, and in some cases, inhibited the reaction somewhat.

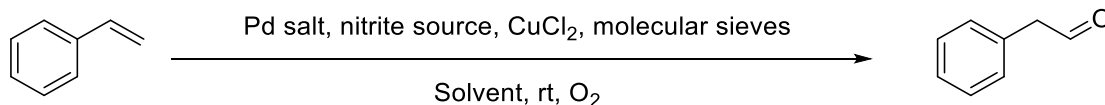
Table 6 - Optimisation based on the modification of the Kang conditions



Entry	CuCl_2 (mol %)	TEMPO (mol %)	Ligand	Temp (deg C)	Ammonia source	Yield (%)	Time (hr)
1	0	0	0	rt	NH_4OAc	0	5
2	0	0	0	rt	NH_4Br	0	4.5
3	0	5	0	rt	NH_4OAc	2	72
4	0	10	0	rt	NH_4OAc	7	72
5	10	10	Bipy (10 mol%)	rt	NH_4OAc	13	24
6	10	10	Bipy (10 mol%)	70	NH_4OAc	9	24

We have also looked at how the AM reaction could be improved compared to the current state-of-the-art, and investigations turned to optimising the AM step. The reactions were limited to one hour so the reactions couldn't go to completion, thus the yield in that limited time frame gave a clear comparison on the effect of changing the reaction conditions. Solvents were changed, the addition of ligands, changing the Pd salt or utilising complexes and the use of molecular sieves were key amendments to the Grubbs or Kang methods. None of the above increased the aldehyde selectivity significantly. Aldehyde selective results occurred from replication of literature conditions (**Table 4, entries 1 and 2**). The addition of MeNO_2 to the Kang reaction mixture had no greater effect on the aldehyde selectivity (**Table 4, entry 4**). The MeNO_2 did however speed up the reaction, achieving the same selectivity but in a third of the time. When aspects of both the Kang and Grubbs methods were combined it was found that the reaction was faster delivered a higher yield. The addition of molecular sieves, however, seemed to close down the system, the with appearance of palladium black apparent in the reaction mixtures. **Table 4, entries 5,6 & 7** demonstrate the similar trends to the reactions without molecular sieves but with much lower yields.

Table 7 - Aldehyde selective anti-Markovnikov oxidation reactions, based on previous literature conditions, combining aspects of the literature conditions and the addition of molecular sieves.

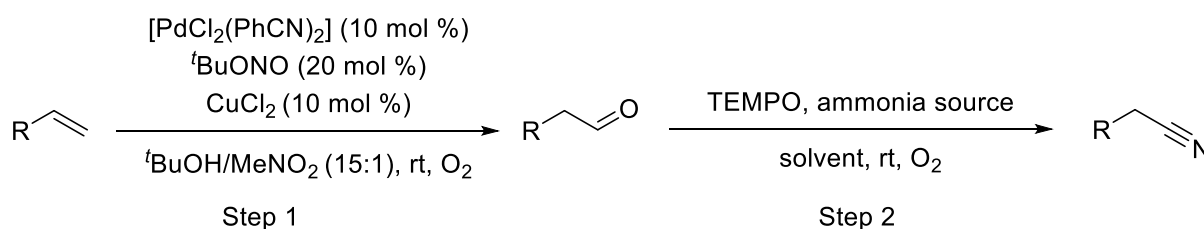


Entry	Method	Pd salt	Nitrite source	CuCl ₂ (mol %)	Solvent	Selectivity (aldehyde)	Molecular sieves	Aldehyde (%)	Time (hr)	Conversion (%)
1	Grubbs	PdCl ₂ (PhCN) ₂ (12 mol %)	AgNO ₂ (6mol%)	12	tBuOH/MeNO ₂ (15:1)	17.8	0	71	6	99
2	Kang	PdCl ₂ (PhCN) ₂ (10 mol %)	^t BuONO (20mol%)	0	tBuOH	2.75	0	11	3	27
3	Hybrid	PdCl ₂ (PhCN) ₂ (10 mol %)	^t BuONO (20mol%)	10	tBuOH/MeNO ₂ (15:1)	19.5	0	39	1	50
4	Kang	PdCl ₂ (PhCN) ₂ (10 mol %)	^t BuONO (20mol%)	0	tBuOH/MeNO ₂ (15:1)	2.75	0	11	1	18
5	Grubbs	PdCl ₂ (PhCN) ₂ (12 mol %)	AgNO ₂ (6mol%)	12	tBuOH/MeNO ₂ (15:1)	4.3	3Å	13	1	21
6	Kang	PdCl ₂ (PhCN) ₂ (10 mol %)	^t BuONO (20mol%)	0	tBuOH	1.5	3Å	3	1	9
7	Hybrid	PdCl ₂ (PhCN) ₂ (10 mol %)	^t BuONO (20mol%)	10	tBuOH/MeNO ₂ (15:1)	3.16	3Å	19	1	33

Conclusions and future work

To summarise, combining aspects of the Grubbs and Kang methods has the potential for a highly aldehyde selective oxidation reaction. If the hybrid method was left to go to completion, after 2 hours, *ca.* 80% aldehyde selective method shows a promising anti-Markovnikov reaction pathway.

The future work would look to optimise this hybrid method and investigate the accessible substrate scope. Once that is achieved, it could be implemented into step 2 in the synthesis of the nitrile. There is still hope that a nitrile selective reaction is possible and that a one-pot two-step method could be developed for synthesis of a nitrile from an alkene.



Scheme 6: The potential for a one-pot two-step reaction of an alkene through to the corresponding nitrile.

References

- (1) J. Smidt, W. Hafner, R. Jira, R. Sieber, J. Sedlmeier and A. Sabel, *Angew. Chem. internat.*, 1962, **1**, 80
- (2) Review on AM Oxidation: J. J. Dong, W. R. Browne and B. L. Feringa, *Angew. Chem. Int. Ed.*, 2014, **53**, 2
- (3) B. L. Feringa, *J. Chem. Soc., Chem. Commun.* 1986, 909
- (4) Z. K. Wickens, B. Morandi and R. H. Grubbs, *Angew. Chem. Int. Ed.*, 2013, **52**, 2
- (5) X. S. Ning, M. M. Wang, X. M. Chen, C. Z. Yao and Y. B. Kang, *Org. Lett.*, 2016, **18**, 2700
- (6) L. M. Dornan, Q. Cao, J. C. A. Flanagan, J. J. Crawford, M. J. Cook and M. L. Muldoon, *Chem. Commun.*, 2013, **49**, 6030
- (7) J. H. Noh and J. Kim, *J. Org. Chem.*, 2015, **80**, 11624



QUILL Quarterly Report

May 2019 – July 2019

Name:	Gareth Nelson		
Supervisor(s):	Dr John Holbrey, Dr Małgorzata Swadźba-Kwaśny		
Position:	PhD Student		
Start date:	13/09/16	Anticipated end date:	30/9/19
Funding body:	DEL		

Ionic Liquid Catalysts for the Glycolysis of PET

Background

There are 4 broad types of PET recycling, primary recycling is pre-consumer scrap recycling. Secondary recycling is physical recycling, this approach first grinds the PET, then melts it before reforming it. The heat and force exerted in this process degrades the polymer leaving it unsuitable for many uses. Tertiary recycling is chemical recycling, the PET is recycled through chemical action, generally through depolymerisation of PET into constituent monomers. These monomers are re-polymerised to regenerate virgin PET. Quaternary recycling is the recovery of energy from the material, this is usually through incineration. This project focuses on chemical recycling of PET as it gives high quality polymers as a product. There are several methods for the depolymerisation of PET, these methods attack the ester linkage to break down the polymer. The use of alcohols (alcoholysis), amines (aminolysis), glycols (glycolysis), or water (hydrolysis) have previously been successful in the depolymerisation of PET. The focus of this project is glycolysis; this occurs through a transesterification reaction between PET and ethylene glycol, commonly catalysed by a metal acetate, carbonate or sulfate. This reaction is attractive because the product, BHET, requires no additional processing before being converted to PET thus is easy to incorporate into PET production. Work utilising ionic liquids as a catalysts was investigated by H, Wang et al.^{1,2} Initially their work utilised imidazolium halide and several acidic ionic liquids, poor yields were achieved but this showed a new approach to the glycolysis reaction.² Q, Wang also utilised ionic liquids as catalysts, previously H, Wang had performed this reaction using [bmim][FeCl₄], the logical extension of this was to test other transition metal salt containing ionic liquids.^{3,4} Q, Wang found that while [bmim][FeCl₄] was effective, [bmim]₂[ZnCl₄] and [bmim]₂[CoCl₄] were more effective, achieving similar conversion of PET (almost 100%) but greater yields of BHET with an increase of almost 20% over [bmim][FeCl₄] for both ionic liquids. Work in literature had previously used acetate ionic liquids, however the results reported were lower and required higher temperatures and more catalyst than those reported by H, Wang using halometallate ionic liquids.⁵

- (1) H. Wang, Y. Lui, Z. Li, X. Zhang, S. Zhang, and Y. Zhang, *Eur. Polym. J.*, 2009, 45, 1535–1544
- (2) H. Wang, Z. Li, Y. Liu, X. Zhang, and S. Zhang, *Green Chem.*, 2009, 11, 1568-1575.
- (3) H. Wang, R. Yan, Z. Li, X. Zhang, and S. Zhang, *Catal. Commun.*, 2010, 11, 763–767.
- (4) Q. Wang, Y. Geng, X. Lu, and S. Zhang, *ACS Sustain. Chem. Eng.* 2015, 3, 340–348
- (5) A.M. Al-Sabagh, F.Z. Yehia, A.M.M.F. Eissa, M.E. Moustafa, G. Eshaq, A.R.M. Rabie, and A.E. El-Metwally *Ind. Eng. Chem. Res.*, 2014, 53, 18443–18451



Objective of this work

The objective of this work is the production of bis(2-hydroxyethyl)terephthalate, a monomeric intermediate in PET production, from the glycolysis of waste PET. To achieve this, the applications of halometallate ionic liquids in the catalysis of the glycolysis of PET will be investigated and the use of acetate containing ionic liquids as catalyst for the glycolysis of PET will be explored.

Progress to date

Work was carried out to repeat experiments for both [bmim][OAc] and [bmmim][OAc] as catalysts across a range of times and temperatures, while results were collected for these reactions recent issues with the HPLC have caused the results to fall far from previous results under the same conditions as well as the results being far lower than would be reasonably expected. Time will be booked on the HPLC in the immediate future along with another fresh calibration curve.

Initially testing of additives for use with [bmim]Cl focused on a few acetate salts. $\text{Sr}(\text{OAc})_2$ and KOAc were the first tested. KOAc was seen to be ineffective on its own at 0.001 mol however $\text{Sr}(\text{OAc})_2$ was found to be very active in this reaction at 0.0005 mol. Due to this result and the prevalence of $\text{Zn}(\text{OAc})_2$ in industrial glycolysis reactions, it was decided to move away from the use of these salts as the lack of activity of KOAc is likely due to the presence of the potassium ion.

To expand the data for a paper that is being written a series of experiments were performed using a different method from my previous work, 185 °C reaction temperature, 1 hour reaction time, 0.2 g catalyst, 1 g PET and 10 g ethylene glycol. The catalysts selected for testing were KOAc, [mmim]Cl, and [mmim]Cl with KOAc. However soon into testing it became apparent that at the high catalytic loadings of this method KOAc was very active. This is in contrast to previous work where it was seen that KOAc on its own was insufficient to initiate the glycolysis reaction. It has become clear that at the catalytic loading I had used prior to these reactions the KOAc was at insufficient concentration to initiate the reaction. Work was recently started investigating the recyclability of using 1,3-dimethylimidazolium-2-carboxylate as a catalyst. A new batch of the carboxylate was produced but the early results diverge greatly from known previous experiments using the same method.

Conclusions and future work

Due to issues with the HPLC most results are being rerun. However the investigation into the use of additives with [bmim]Cl was halted as $\text{Sr}(\text{OAc})_2$ was too reactive towards the glycolysis reaction, additionally KOAc also performs the reaction but required higher catalyst loading. The reactivity of the additives that is required to initiate the carbene formation also means that the additive is reactive enough to perform the transesterification reaction.

Work towards a paper will continue, specifically recycling studies using 1,3-dimethylimidazolium-2-carboxylate.

QUILL Quarterly Report

May 2019 – July 2019

Name:	Zara Shiels/Laura Lytle		
Supervisor(s):	Dr Artioli, Prof Nockemann, Dr Harrison		
Position:	PhD		
Start date:	Feb 2019	Anticipated end date:	2022
Funding body:	Interreg (Renewable Engine Project)		

Developing New Nanocatalysts for the Direct Conversion of Biogenic Carbon Dioxide (CO₂) to Sustainable Fuels

Background

Rising CO₂ emissions, global warming, ocean acidification and a reliance on a diminishing source of fossil fuels are all factors having a detrimental effect on the environment, making our current way of living unsustainable.¹ In recent years, there has been a large emphasis on research that addresses these issues. Global warming is a serious problem and therefore, many governmental protocols and objectives have been put in place to tackle the issue, for example the Kyoto protocol in 1997, the Paris protocol² published in 2015 and the Clean Power Plan (CPP)³ announced by President Obama in 2015. More recently a proposal has been signed to repeal the CPP in 2017, therefore now, more than ever, there needs to be action.⁴ One solution that has been proposed as a means of relinquishing our need for fossil fuels, is to use waste CO₂ from processes (such as anaerobic digestion) and convert this to fuels.

Typically, for gas conversion reactions to occur efficiently, a catalyst is required and in the case of CO₂ conversion to hydrocarbon fuels, iron oxide nanoparticles have exhibited high activities. Furthermore, in a drive to reduce the use of toxic solvents in chemical processes, ionic liquids can be used in the preparation of this catalyst, whilst controlling the size of the nanoparticles without the need for additional capping agents and allows for dispersion which can prevent agglomeration of the particles. Several authors have reported that by employing this synthetic method, a multi-action catalyst was obtained, with three different sites for conversion of CO₂ to hydrocarbons in the C₅-C₁₁ range.^{5,6,7}

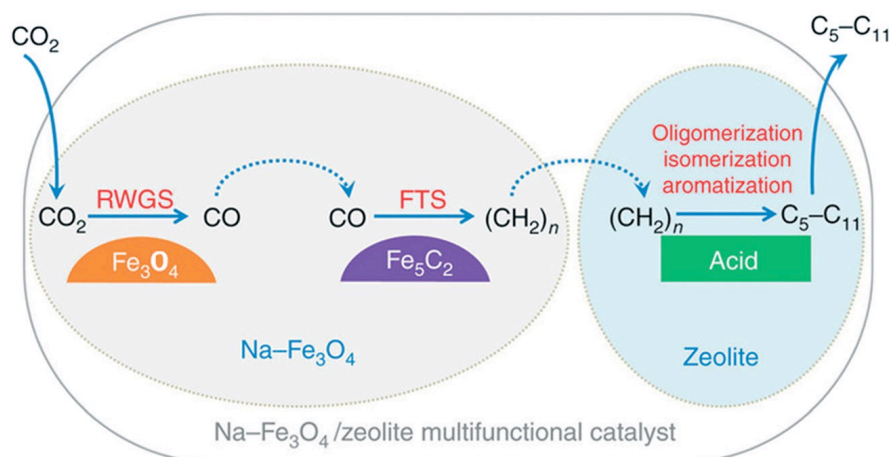


Figure 13 – Depiction of the multifunctional catalyst required for conversion of CO₂ to hydrocarbons



This report proposes two different possible catalyst synthesis routes that utilise these necessary ionic liquids. The first synthesis method involves the thermal decomposition of an iron precursor in a high temperature solution phase reaction. Once the reaction is complete, the produced iron (III) oxide can be separated through decantation and washed with hexane. Once fully separated, the iron (III) oxide will then be embedded within a zeolite structure for pH control and as a solid support for the final catalyst

The second novel method involves use of two iron precursors, already in the desired oxidation states, heated while stirring in the presence of a specifically chosen ionic liquid and requires less energy than previously reported syntheses. Through varying the ionic liquid utilised as the reaction solvent it is hoped we can achieve the capping capabilities of the previous reaction without the need for additional reagents.

Characterisation will be carried out at each stage of the process by a variety of methods: Nuclear Magnetic Resonance (NMR) Spectroscopy, Powder X-Ray Diffraction (PXRD), Temperature Programme Reduction (TPR), Scanning Electron Microscopy (SEM), Transmission Electron Microscopy (TEM), Brunauer-Emmett-Teller (BET) Surface Area analysis and so on.

Objective of this work

The overall aim of this project is to develop a reproducible method of synthesising a nanocatalyst for conversion of CO₂ to sustainable fuels. Synthesis and use of different ionic liquids in the preparation of the Fe₃O₄ catalyst will be carried out, as well as varying the zeolite support used, characterisation and finally high pressure testing under reaction conditions. A control will also be prepared in order to compare the novel catalyst with a conventional method.

Progress to date

The precipitation method involves first adding hydrated iron chlorides to a diluted solution of hydrochloric acid. Following this stage, dropwise addition of a precipitating agent results in the formation of a black precipitate of iron (II,III) oxide. Adequate control of the pH of the reaction mixture allows for the formed iron (II,III) oxide precipitate to remain in solution at around pH 10. Due to the magnetic nature of the produced iron (II,III) oxide nanoparticles, commonly referred to as '*Magnetite*', separation can be achieved through the use of a strong neodymium magnet.

Initially the precipitation method, as described above, was undertaken to be used as a comparison to the catalyst synthesised using both ionic liquid methods. This was successfully achieved, creating 3 different samples of high sodium, low sodium and no sodium content. These samples were then studied under XRD analysis as shown in **Figure 2**. The Scherrer calculator was used to find the average particle size which was 6.3 nm. Initially the samples were attempted to be pelleted at 30MPa and sieved to 20-40 meshes. However this was only achieved with one sample due to the zeolite powder being too fine for the presses. More of this sample was produced and tested against simple ball-milling to combine the iron oxide nanoparticles and zeolite. After analysis it was found that ball-milling method compared to pelleting and sieving made to difference to nanoparticle size or surface area.

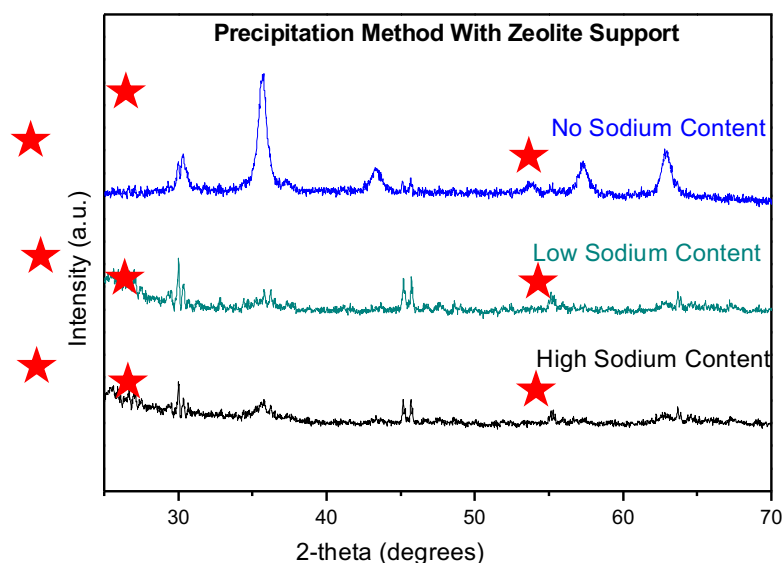


Figure 2 - XRD analysis of each precipitation method embedded on zeolite support.

Temperature-programmed reduction (TPR) is a widely used tool for the characterization of metal oxides dispersed on a support, in this case iron oxide on a zeolite support. The TPR method yields quantitative information of the reducibility of the oxide's surface, as well as the heterogeneity of the reducible surface.

TPR analysis has been carried out on each method of iron oxide synthesis in order to compare and contrast the reducibility of each catalyst. The TPR analysis for each type of precipitation method is shown in **Figure 3** below.

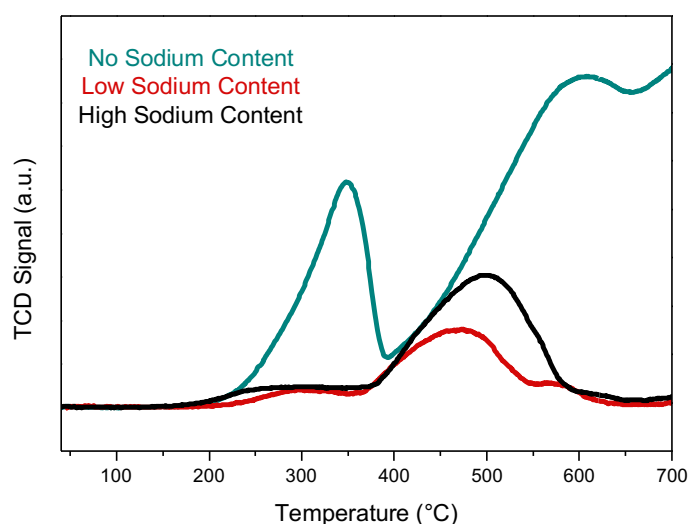


Figure 3 - showing TPR analysis for each precipitation method.

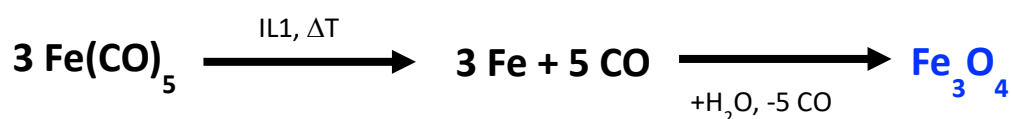
From this analysis we can construct table 1 to determine at which temperatures each sample reduces.

Table 1- Showing temperatures at which iron oxide reduces at each stage

Fe ₃ O ₄	FeO	Fe
No Sodium	347°C	588°C
High Sodium	288°C	497°C
Low Sodium	300°C	474°C

Method 1 involving 1 iron precursor was investigated. This synthesis involved 1 ml of iron precursor Fe(CO)₅ being added to a 100 ml round bottom flask containing 25ml of ionic-liquid [Bmim][BF₄] and 1.9ml of Oleic Acid. Stabilizing agents were added in the following quantities; Oleylamine (0.3ml) and Hexadecanediol (2.7g). The reagent mixture is heated to 280°C over a period of 2 hours then kept at constant temperature for a further hour and stirred vigorously using a magnetic stirrer. The newly formed dark black solution was then washed 3 times with 25ml of Dichloromethane (DCM) and allowed to stand over a neodymium magnet for 30 mins. The black ferrous fluid is pulled out of suspension and the remaining solvent layer decanted.

The Ferrous liquid is once again washed with methanol and decanted. The wet black solid is then dried in an oil bath at 50°C under vacuum for 24 hours. Solid Iron oxide can then be extracted. The balanced symbol equation for the reaction is shown below:



The sample was then ball milled with zeolite on a 1:1 mass ratio. The XRD analysis of this sample is shown in **Figure 3** below.

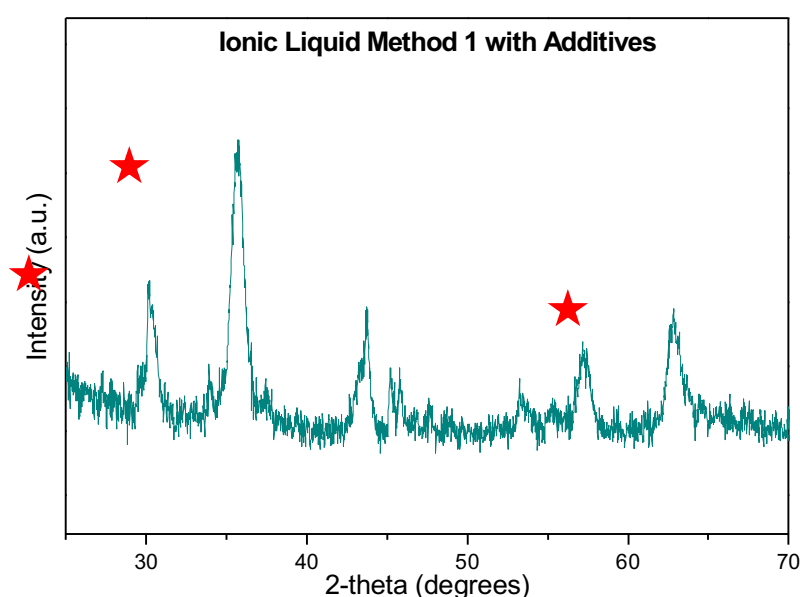


Figure 4 - XRD analysis of method 1 with additives on zeolite support.

The average particle size was found to be 6.3nm. TPR analysis was also undertaken for this sample, this analysis is shown in **Figure 5**.

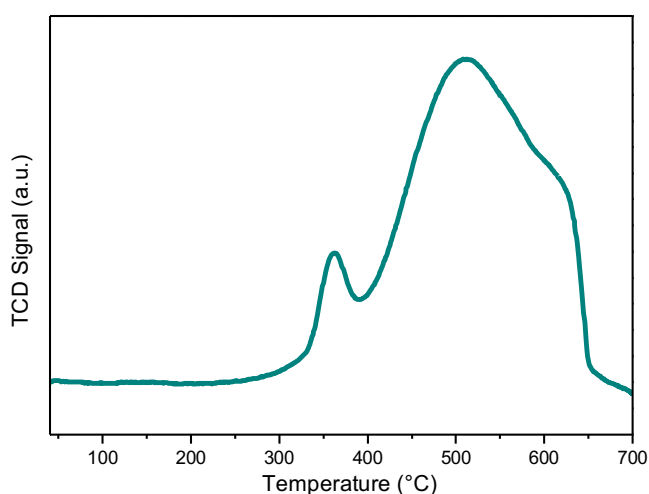


Figure 5 - showing TPR analysis for Method 1 with additives.

From this analysis it is concluded that the Fe_3O_4 particles reduce to FeO at 360°C and further reduce to Fe at 510°C.

Method 2, a method being developed by Queens University Belfast has also successfully produced iron oxide nanoparticles. It has been tested with and without NH_3 , the later giving a yield of 70.8%. The isolation of this solid has been fully optimised with the washing of water and ethanol and repeated centrifuging and suction filtering with hopes of higher yields of both methods being established currently. Both have undergone calcination at 420°C under nitrogen. PXRD analysis of before and after calcination is shown in **Figure 6** and **Figure 7** below.

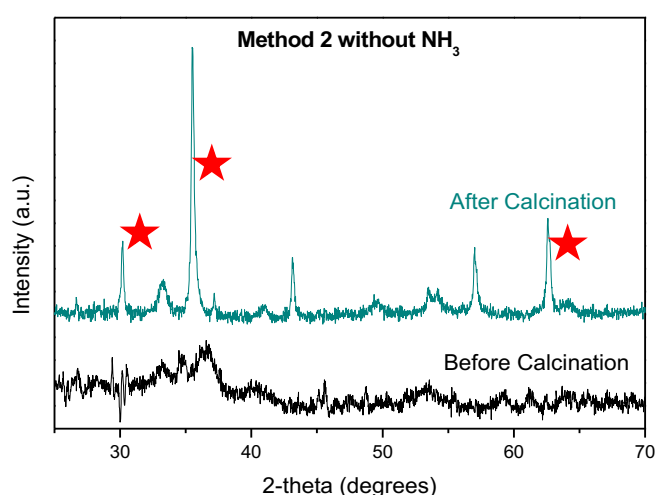


Figure 6 - XRD analysis of method 2 without NH_3 addition before and after calcination

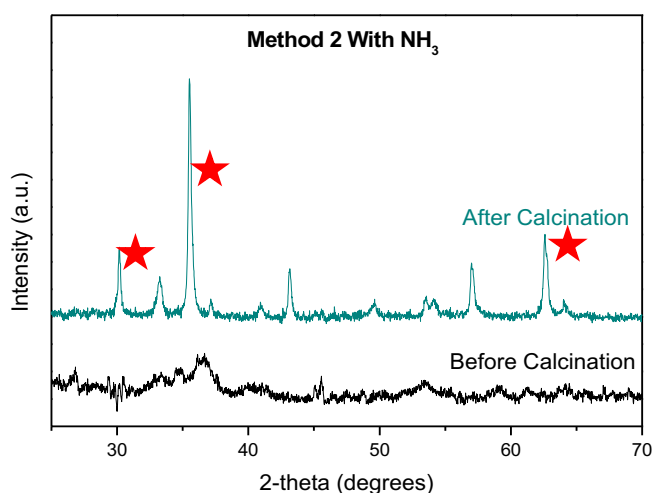


Figure 7 - XRD analysis of Method 2 with NH_3 before and after calcination.

Investigation is underway on pH control of both with and without ammonia to optimise the morphology of the catalyst produced. TPR analysis was carried out on each sample before and after calcination, this is shown in **Figure 8** and **Figure 9**.

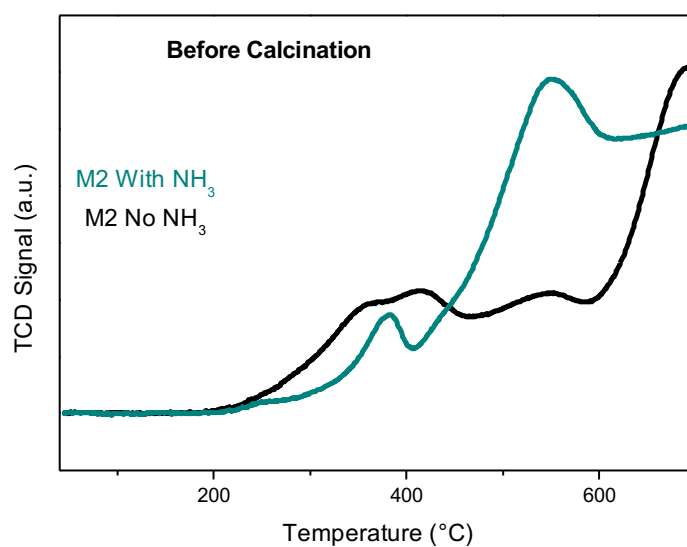


Figure 8 - TPR analysis of Method 2 with and without NH_3 before calcination.

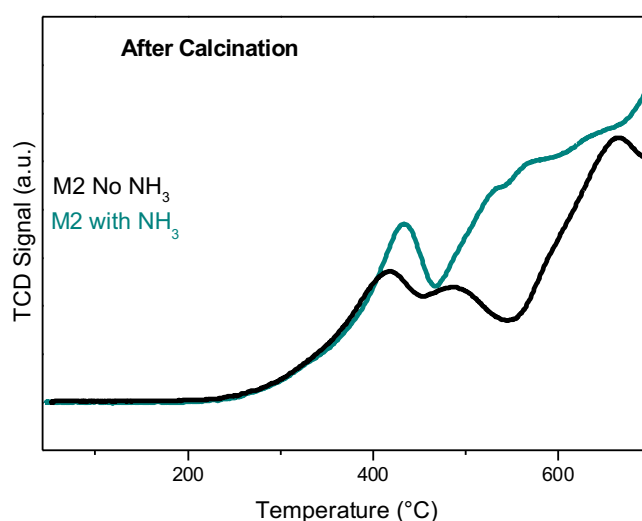


Figure 9 - TPR analysis of Method 2 with and without ammonia after calcination.

From this **Table 2** can be presented showing the different reduction temperatures of each sample.

Table 2- Showing reduction temperatures of method 2 samples with and without NH_3 before and after calcination.

	Before Calcination		After Calcination	
	FeO	Fe	FeO	Fe
Without NH_3	410°C	693°C	416°C	663°C
With NH_3	385°C	510°C	425°C	??

An overall comparison of each sample is shown in **Figure 10** and from this is can be concluded that the catalysts that have been prepared using ionic liquid synthesis show a higher reducibility to those synthesised using the precipitation method.

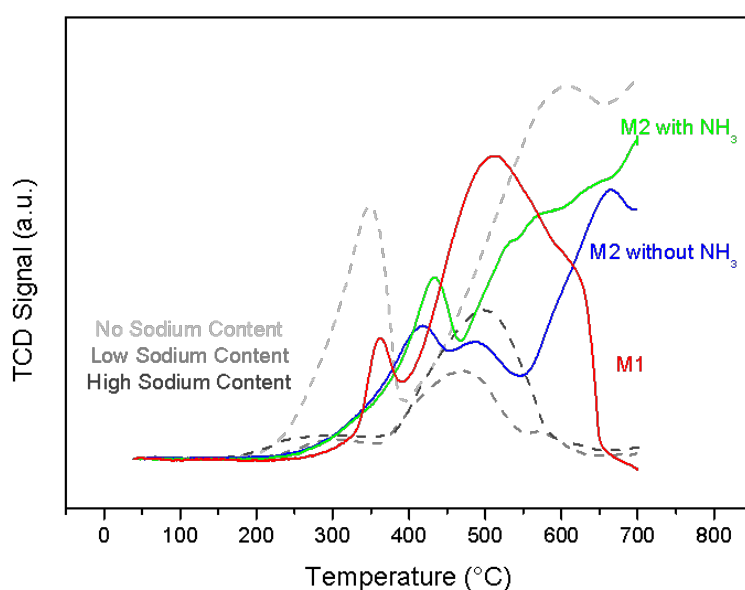




Figure 10 - Comparison of each TPR analysis for each sample.

Conclusions and future work

In conclusion the precipitation method as described above has been successfully reproduced from literature and used as a comparison for the new methods introduced using ionic liquids. The method proposed by Wang et al. has been successfully prepared and compared with the novel method proposed herein at QUB. Method 2 proposed at QUB has been optimised producing much higher yields of >70% and is also a much less energy intensive method of producing the iron oxide nanoparticles. After TPR analysis it has been found that both ionic liquid methods show higher reducibility than the conventional precipitation method with method 2 reducing at higher temperatures than that of method 1.

Future work will include the testing the activity of the catalyst in producing hydrocarbons of chain length C_5 - C_{11} will be shown by use of a reactor for hydrogenation of CO_2 which is connected to a Gas Chromatograph (GC) with a specific column for detection of olefins in this chain length range. Recycling of the ionic liquid used in method 2 will also be attempted to achieve a more environmentally friendly synthesis. The pH of the reaction in method 2 will be closely monitored to optimise the morphology of the catalyst produced.

References

- (1) J. Wei, Q. Ge, R. Yao, Z. Wen, C. Fang, L. Guo, H. Xu and J. Sun, *Nature Communications*, 2017, 8, 15174.
- (2) Ce. Croopmémenittee, 2.
- (3) The Clean Power Plan, <https://www.edf.org/clean-power-plan-resources>, (accessed 12 March 2019), 2016, 290.
- (4) H. Yang, C. Zhang, P. Gao, H. Wang, X. Li, L. Zhong, W. Wei and Y. Sun, *Catal. Sci. Technol.*, 2017, 7, 4580–4598.
- (5) I. Dimitriou, P. García-Gutiérrez, R. H. Elder, R. M. Cuéllar-Franca, A. Azapagic and R. W. K. Allen, *Energy & Environmental Science*, 2015, 8, 1775–1789.
- (6) M. D. Porosoff, B. Yan and J. G. Chen, *Energy & Environmental Science*, 2016, 9, 62–73.